NACA

RESEARCH MEMORANDUM

FLIGHT INVESTIGATION OF A SUPERSONIC PROPELLER

ON A PROPELLER RESEARCH VEHICLE AT MACH

NUMBERS TO 1.01

By Jerome B. Hammack, Max C. Kurbjun,
and Thomas C. O'Bryan

Langley Aeronautical Laboratory
Langley Field, Va.

CLASSIFIED DOCUMENT

NATIONAL ADVISORY COMMITTEE
FOR AERONAUTICS
WASHINGTON
July 10, 1957

NATIONAL ADVISORY COMMITTEE FOR AERONAUTICS

RESEARCH MEMORANDUM

FLIGHT INVESTIGATION OF A SUPERSONIC PROPELLER

ON A PROPELLER RESEARCH VEHICLE AT MACH

NUMBERS TO 1.01

By Jerome B. Hammack, Max C. Kurbjun,
and Thomas C. O'Bryan

SUMMARY

A description is given of an NACA propeller research vehicle, the
McDonnell XF-88B airplane, capable of testing governing propellers up to
and slightly above Mach numbers of 1.0. Altitudes up to 40,000 feet are
attainable. Propellers up to 10 feet in diameter can be tested with a
maximum power input of 2,500 brake horsepower at two rotational speeds.
The airplane is instrumented to obtain aerodynamic and structural data.

Results are given of a flight investigation made with this vehicle
to determine the aerodynamic characteristics of a supersonic propeller
at speeds up to a flight Mach number of 1.01. The propeller was designed
for a flight Mach number of 0.95, an advance ratio of 2.2, and a power
coefficient of 0.22. At the design flight Mach number of 0.95, the pro-
peller efficiency was measured to be 79 percent. At the maximum obtained
Mach number of 1.01, the efficiency was 78 percent. Thrust distributions
obtained by the use of a slipstream survey rake were of a uniform nature
and showed no discontinuity typical of subsonic propellers when operated
under conditions which produce sonic local conditions. Limited theoretical
calculations of efficiency indicate good agreement with the test results.

INTRODUCTION

Several years ago the National Advisory Committee for Aeronautics
realized there was a need for providing continuous research on propel-
lers designed for high efficiency for airplanes of maximum range at
speeds up to Mach number 1.0. These propellers would be utilized on
airplanes on which range and efficiency of operation were paramount,
such as long-range strategic bombers, tankers, long-range assault trans-
ports, maximum-endurance tactical-fighter bombers, and passenger trans-
ports. In order to study the problem as a whole, including operation

under installation conditions with a turbopropeller engine providing the driving power, a propeller flight-research program was planned. The airplane chosen for this study was a McDonnell XF-88 turbojet airplane. The research program is a joint Air Force-Navy-NACA effort. The airplane and continuing propeller research equipment are supplied by the U. S. Air Force. The Department of the Navy supplies the turbojet and turboprop engines. The research program and its execution are the responsibility of the NACA.

The planned propeller research program in which the XF-88B propeller research airplane is used is composed of several phases and is an outgrowth of a comprehensive study of conditions affecting propellers operating at transonic speeds for purposes of maximum range. These conditions include both structural and aerodynamic factors. Some of the phases planned for investigation are tests of propellers designed for flight Mach numbers around 0.9 and an advance ratio around 2.0, tests to study the effects of variation in blade root thickness ratio, tests to study the effect of blade shock interference, and tests to study effects of variation in design advance ratio. Early in the preliminary phases of the research program it was considered desirable to investigate first the effects of changes in the design advance ratio upon propeller efficiency and power absorption. Consequently, the first propeller of the investigation is a supersonic propeller having an advance ratio of 2.2; the preliminary results of tests with this propeller are presented in references 1 and 2. The primary aerodynamic results of the flight investigation of the advance-ratio-2.2 supersonic propeller are presented herein together with a description of the vehicle.

SYMBOLS

A   area of propeller disk, sq ft

b   blade chord, ft

c_p specific heat at constant pressure, 6,006 ft-lb/slugs/$^\circ$F

c_l section lift coefficient

c_d blade section drag coefficient

$c_{d,f}$ section friction drag coefficient

$c_{d,i}$ section induced drag coefficient

C_P propeller power coefficient, $P/\rho n^3 D^5$

C_T propeller thrust coefficient, $T/\rho n^2 D^4$

C_T' propeller-thrust-coefficient correction due to slipstream rotation

D   propeller diameter, ft

g   acceleration due to gravity, 32.2 ft/sec^2

h   blade thickness, ft

H   total pressure, lb/sq ft

J   propeller advance ratio, V/nD

L/D   lift-drag ratio

M   free-stream Mach number

n   propeller rotational speed, rps

p   static pressure, lb/sq ft

P   power, ft-lb/sec

r   radius of an element on blade from center line of rotation, ft

r_s radial dimension to survey measurement, ft

R   gas constant, 53.3

t   free-stream static temperature, $^\circ$F abs

T   thrust, lb

V   velocity, ft/sec

$x = 2r/D$

$x_s = 2r_s/D$

α angle of attack of blade section, deg

β blade angle, deg

γ	ratio of specific heats
ΔH	total-pressure rise in slipstream, lb/sq ft
$\Delta\theta$	stagnation-temperature rise in propeller slipstream, $^\circ$F
η	propeller efficiency
ρ	density of air, slugs/cu ft
ϕ	angle of advance, $\tan^{-1} J/\pi x$, deg
ψ	angle of rotation of slipstream, deg

Subscripts:

l	local conditions
∞	free-stream conditions
t	propeller tip condition

APPARATUS

The Propeller Research Vehicle

Shown in figure 1 is a view of the McDonnell XF-88B propeller research vehicle. This airplane is able to fly at Mach numbers in excess of 0.9 in level flight and is capable of exceeding Mach number 1.0 in dives.

General characteristics.- The general characteristics of the propeller research vehicle are as follows:

```
Span, ft . . . . . . . . . . . . . . . . . . . . . . . . . . . . . . 39.7
Length, ft . . . . . . . . . . . . . . . . . . . . . . . . . . . . . . 58
Wing area, sq ft . . . . . . . . . . . . . . . . . . . . . . . . . . . 350
Sweepback at quarter chord, deg . . . . . . . . . . . . . . . . . . . 35
Wing aspect ratio . . . . . . . . . . . . . . . . . . . . . . . . . . 4.49
Weight (approximately, depending upon propeller
   configuration), lb . . . . . . . . . . . . . . . . . . . . . . . 22,000
Fuel capacity, lb . . . . . . . . . . . . . . . . . . . . . . . . . 3,550
Flight endurance time (approximately), min . . . . . . . . . . . . . 45
Main power plant . . . . . Two Westinghouse J34-WE-34 plus afterburners
Propeller power plant . . . . . . . . . . . . Allison XT38-A-5 turboprop
Turbojet thrust at take-off (two engines), lb . . . . . . . . . . 6,600
Turboprop power at sea level, shp . . . . . . . . . . . . . . . . 2,500
```

Propeller rotational speeds available at 100-percent
   engine speed, rpm . . . . 1,700 and 3,600
Maximum propeller diameter available for test, ft 10

Propeller drive system.- The engine that drives the test propellers
is an Allison XT38-A-5 turboprop engine which has the commercial designa-
tion of Model 501-F1. This basic power plant and later versions are used
in several present-day airplanes. The power section includes a single-
entry multistage axial-flow compressor, a set of eight combustion chambers,
and a four-stage turbine. The special gearbox provides two propeller
rotational speeds of 1,700 rpm and 3,600 rpm at a power section rotational
speed of 14,300 rpm. Either of these propeller rotational speeds can be
made available by selection of gear sets during the gearbox assembly.
Figure 2 shows the power section and this special gearbox. The gearbox
weighs 445 pounds in the 1,700 rpm assembly and 350 pounds in the 3,600 rpm
assembly; the difference in weight is caused by the elimination of the
planetary system in the gearbox used for a speed of 3,600 rpm.

The propeller hub assemblies to which the research blades are fitted
are electrically controlled. The hub provides for a rate-of-pitch change
of a maximum of 2° per second with a range from flat pitch to feather.
The selection of these assemblies was based on the following main factors:
(1) maximum available blade retention capacity to provide maximum latitude
in blade design; (2) maximum blade-twisting-moment capacity to provide
maximum latitude in blade design; (3) minimum hub diameter; and (4) ade-
quate hub rear extension to provide space for a spinner thrust isolation
bearing between the pitch controls and gearbox. These factors are out-
lined in reference 3. The design strengths of the propeller hubs are
outlined in reference 4.

The signals supplied to the electric motor that change the blade
pitch are furnished by an electronic governor. Details of the electronic
governor are outlined in reference 3, as mentioned previously. Various
time constants have been provided to be used with the electronic governor;
the time constant used depends on the propeller being tested. These time
constants refer to the response of the blades to the change in rotational
speed.

Test Propeller

Aerodynamic and structural considerations underlying supersonic pro-
peller design are outlined in several reports, for instance, references 5,
6, and 7. The supersonic propeller of this investigation is designed for
a forward Mach number of 0.95 and a power coefficient of 0.22. Since the
propeller is a supersonic type, it is designed for optimum profile effi-
ciency and the design advance ratio (2.2) is such that the propeller
operates at an optimum advance angle in keeping with the fact that profile

efficiency is a maximum at an angle of advance of about 45°. This design procedure produces higher rotational speeds than those of conventional propeller design and requires low thickness ratios, as low as is consistent with structural integrity.

The supersonic propeller is a model of the Aeroproducts 12-foot-diameter propeller that was designed to absorb 7,500 horsepower in its full-scale version. The propeller is a three-blade configuration with a 7.2-foot diameter. The blades were fabricated from solid steel having an ultimate tensile strength of 180,000 pounds per square inch. The propeller has NACA 16-series symmetrical airfoil sections with a tapered plan form from 11.1-inch root chord to an 8.4-inch tip chord. The thickness ratio varies from 6 percent at the spinner juncture to 2 percent at the tip. The blade-form curves are shown in figure 3. The vibratory bending and torsional characteristics of this propeller were given in reference 1. The propeller was tested in conjunction with a 41° conical spinner which was sealed at the base but open at the blade juncture, as shown in figure 1.

INSTRUMENTATION AND DATA REDUCTION

The XF-88B airplane is instrumented to gather aerodynamic and structural information concerning the propeller undergoing investigation. Quantities measured produce the following information: Power, thrust, propeller efficiency, root blade angles, bending stresses, steady and vibratory, torsion stresses, steady and vibratory, and rotational speed. Along with this, certain measurements of general information are recorded, such as airspeed, Mach number, free-air temperature, throttle and governor control position, altitude, normal acceleration and longitudinal acceleration. A schematic drawing showing the instrumentation is presented in figure 4.

Power Measurements

The power input to the propeller gearbox is measured by an Allison torquemeter. A cutaway drawing of this torquemeter is shown in figure 5. The torquemeter was originally designed as a commercial unit for a 4,000-horsepower turbine engine. Although adequate for the original intent the unit required extensive modification before it was suitable as a research tool on the XF-88B propeller research airplane. A complete description of the modified torquemeter unit is contained in appendix A. Power is considered to be accurate to ±20 horsepower or a ΔC_p of 0.003 at 30,000 feet.

Thrust

Propeller thrust is measured by a slipstream survey rake in a manner described in reference 8. Incremental or section values may be used directly or, if total thrust is desired, integrated from the fuselage surface to the rake station showing zero incremental thrust. The survey rake used on the XF-88B propeller research airplane is shown in figure 6 and details of a probe are shown in figure 7. This probe measures total-pressure rise and static pressure. The reference total-pressure tube is at the extreme end of the survey rake out of the influence of the pro-peller slipstream. Recording manometers register the difference in total-pressure rise between each probe and the reference probe. This total-pressure rise is a function of propeller thrust.

Incremental thrust was determined from measurements of total-pressure rise in the slipstream in conjunction with free-stream conditions. From reference 8 the equation for thrust is

$$dT = 7p_l \left[\left(\frac{H_l}{p_l} \right)^{2/7} - 1 \right] \left[\frac{\left(H_l^{2/7} - p_\infty^{2/7} \right)^{1/2} - \left(H_\infty^{2/7} - p_\infty^{2/7} \right)^{1/2}}{\left(H_l^{2/7} - p_l^{2/7} \right)^{1/2}} \right] dA \quad (1)$$

Under conditions of survey covered by this paper this equation can be reduced to the short-form equation, also found in reference 8:

$$dT = \left(\frac{p_\infty}{H_\infty} \right)^{5/7} \Delta H \, dA \quad (2)$$

or

$$\frac{dT}{d\left(x_s^2 \right)} = \pi \left(\frac{D}{2} \right)^2 \left(\frac{p_\infty}{H_\infty} \right)^{5/7} \Delta H \quad (3)$$

and in thrust-coefficient form

$$\frac{dC_T}{d(x_s^2)} = \frac{dT/d(x_s^2)}{\rho n^2 D^4} = \frac{\left(\frac{p_\infty}{H_\infty}\right)^{5/7} \Delta H}{4\rho n^2 D^2} \tag{4}$$

Values of section thrust coefficient were calculated for a few cases by both the short-form and long-form equations and were compared and found to agree within the accuracy of the measurements. Consequently, the remainder of the section thrust coefficients are calculated by the short-form equation. The thrust distribution determined from the slipstream survey is considered to be accurate to ±2.0 percent.

The total thrust coefficient was determined from integration of the total-pressure rise in the slipstream in conjunction with free-stream conditions for both the left and right rakes and then averaging these two values. Thus, the equation for the thrust coefficient is the integral of equation (4) or,

$$C_T = \frac{\pi \left(\frac{p_\infty}{H_\infty}\right)^{5/7}}{4\rho n^2 D^2} \int \Delta H d(x_s^2) \tag{5}$$

Inasmuch as the total-pressure probes are insensitive to small changes in angle, the thrust calculated in this fashion does not account for rotation of the slipstream. A correction for slipstream rotation (discussed in ref. 9) was made. This correction is a function of section power which was determined by measurement of slipstream-stagnation-temperature rise as outlined in reference 4. This correction averages about 5 percent.

Efficiency

Propeller efficiency is the ratio of thrust produced to power absorbed multiplied by the true speed of the airplane:

$$\eta = \frac{T}{P} V_\infty \tag{6}$$

In terms of nondimensional coefficients, equation (6) is expressed as

$$\eta = \frac{C_T}{C_P} J \qquad (7)$$

The efficiency measurements reported herein are considered to be accurate to ±3 percent.

Blade Angle

Blade angles are indicated by a precision blade-angle indicator which was manufactured by the Propeller Division of Curtiss-Wright Corporation and which consists of a propeller-hub-mounted transmitter unit geared to the propeller blades through the propeller power gear, airplane-mounted electronic amplifier, and both a recording and panel-mounted visual indicating instrument. The recording instrument was provided by the NACA. The blade-angle readings may be repeated to within ±0.1°. A complete description of this precision blade-angle instrument is available in reference 10.

The remaining general instrumentation is standard NACA flight-research instrumentation.

Test Procedure

The normal flight procedure is generally as follows: The airplane is towed to the end of the runway, clearance is obtained from the tower, and the J-34 jet engines are started, checked, and afterburners fired for take-off. In order to conserve fuel the afterburners are cut off and the T-38 turboprop started at an altitude of 5,000 feet to assist in the climb.

Level-flight Mach numbers up to approximately $M = 0.9$ can be obtained by using both the J-34 turbojet engines with afterburners and the T-38 turboprop engine. Mach numbers up to and slightly above 1.0 can be obtained in pushovers to dives of 30° from 40,000 feet.

Data are continuously recorded as the pilot accelerates from 0.5 Mach number up to the maximum test Mach number. The profile of a typical test shows a level-flight acceleration up to $M \approx 0.9$, followed by a dive to the maximum Mach number obtainable.

RESULTS AND DISCUSSION

Thrust Distributions

Thrust distributions for the entire range of test Mach numbers are shown in figure 8 and are presented as variations in total pressure with radial stations for both left and right survey rakes. These total-pressure distributions indicate a smooth uniform distribution with no breakdowns in the outboard regions which are characteristic of subsonic propellers encountering compressibility losses. This is due to the fact that operation has already passed into the supercritical region over the entire propeller. For example, the tip Mach number at a design Mach number of 0.95 is approximately 1.6. The thrust distributions are presented to show the behavior of a supersonic propeller through the Mach number range of test. It is to be noted that the incremental thrust extends past the propeller tip station $(x_s{}^2 = 1.0)$; this extension is due primarily to the expansion of the air mass by the conical fuselage and spinner.

Shown in figure 9 are the two typical thrust distributions computed from the measured total-pressure distributions by use of the short-form equation (eq. (4)). These curves again reflect the uniform distribution of total pressure as measured by the slipstream survey rakes.

The characteristic difference in thrust-distribution levels between the right and left survey rakes is shown in figures 8 and 9 and is a result of inclination of the thrust axis. The decrease in difference between right and left thrust distributions as Mach number increases (fig. 8) is representative of the decrease in angle of inclination of the thrust axis, which reflects the usual decrease in angle of attack of the airplane with increasing Mach number. The difference continues to decrease until at $M = 0.85$ the two surveys are nearly coincident; this agreement indicates near zero angle of inclination of the thrust axis. At $M = 0.90$ the survey distributions cross over, that is, the left distribution is higher than the right and a negative angle of inclination of the thrust axis is therefore indicated. Further increase in Mach number to $M = 0.95$ results in the recrossing of the survey distributions and again a positive angle of inclination is indicated. The variation of thrust axis angle indicated by the survey distributions is in agreement with the measured angle variations in reference 1.

Variation of Aerodynamic Characteristics

With Mach Number

Shown in figure 10 are the variations in propeller efficiency, power absorbed, advance ratio, and thrust coefficient with forward flight

Mach number for five different tests at constant propeller rotational speed of 3,500 rpm. Variations in ambient temperatures show up as changes in advance ratio and power coefficient at a given Mach number. The variation in propeller efficiency with flight Mach number is comparatively flat, being about 80 percent at Mach number 0.70 and dropping off slightly as the speed is increased to M = 1.01. It is interesting to note that the propeller efficiency at the highest flight Mach number of measurement - that is, Mach number 1.01 - is 78 percent. At the design advance ratio of 2.2, and Mach number 0.95 the propeller efficiency shows an average value of 79 percent.

Installation Effects

Interference effects of spinners on the operation of propellers is an important parameter influencing the flow through the plane of the propeller. An investigation of the flow around a conical spinner was reported in reference 11. The tests were made with a dummy nonrotating spinner of the same design as was used on the XF-88B airplane in the tests described herein and under similar flight conditions as those of the present investigation. Reference 11 and unpublished data indicate a reduction in the flow velocity in the plane of the propeller in the neighborhood of 15 percent at forward Mach numbers around 0.95. It is believed that this reduction in air-flow velocity prevents any occurrence of shock interference between adjacent blades, although the propeller of this investigation is operating in a region where it would be expected to come under the influence of shock interference. Figure 11 shows the variation in blade angle, rotational speed, and Mach number during a typical flight. As can be seen, the value of blade angle minus the geometric helix angle is fairly uniform and shows no abrupt increase as might be expected if trailing blade shocks should start destroying the lift on adjacent blades. Point-by-point analysis of every flight, analyzed in the manner shown in figure 11, indicates no evidence of this shock interference. Reference 12 presents a discussion of the shock-interference problem as applied to propellers.

Comparison of Experimental Results With Theoretical

Calculations and Other Data

Figure 12 presents some comparisons of the measured propeller efficiencies with theoretical calculations and with unpublished experimental wind-tunnel data obtained by Cornell Aeronautical Laboratory on a 4-foot-diameter version of the propeller discussed herein. Figures 12(a) and 12(b) show a comparison at forward Mach numbers of 0.85 and 0.90, respectively, for which data are available from the Cornell Laboratory. These data are plotted as propeller efficiency against advance ratio. Figure 12(c) presents the flight-measured efficiencies and theoretical

calculations at a Mach number of 0.98. No data are available from the
Cornell Laboratory at this Mach number. One set of theoretical calcula-
tions was made by Aeroproducts, the designers of the blade, and one set
was made by the authors of this report. The calculations made by Aero-
products are outlined in references 13 and 14 in which an efficiency
loss for shock interference was included in the region wherein shock
interference might be expected. The authors' calculations were made by
use of strip theory and did not include any loss due to shock interference.
The calculations assumed operation at peak efficiency. Airfoil section
characteristics for use in the strip calculations were calculated by
Ackeret's second-order theory modified to account for thickness ratio.
The equations used for calculating these data in the attached shock-flow
region are as follows:

$$c_l = \frac{4\alpha(1 - 2.5h/b)}{\sqrt{M^2 - 1}} \tag{8}$$

$$c_d = c_{d,l} + c_{d,0} + c_{d,f} \tag{9}$$

$$c_d = \frac{4\alpha^2(1 - 2.5h/b)}{\sqrt{M^2 - 1}} + \frac{16}{3}\frac{(h/b)^2}{\sqrt{M^2 - 1}} + c_{d,f} \tag{10}$$

$$\left(\alpha_{max\ L/D}\right)^2 = \frac{c_{d,0} + c_{d,f}}{c_l} \tag{11}$$

$$\left(\alpha_{max\ L/D}\right)^2 = \frac{\frac{16}{3}\left(\frac{h}{b}\right)^2 + 0.005\sqrt{M^2 - 1}}{4(1 - 2.5h/b)} \tag{12}$$

where $c_{d,f}$ is assumed equal to 0.005. From these equations the lift
coefficient for maximum L/D as well as the L/D can be calculated.
In the region where these equations cannot be applied, data have been
obtained from the Langley 24-inch high-speed-tunnel experimental results,
some of which have been published in reference 15. The alteration in
the flow velocity caused by the conical spinner (ref. 11 and unpublished
data) is also included in the calculations and is shown in figure 13.

This alteration amounted to a reduction in section Mach number which, of course, is reflected as an increase in lift-drag ratio. This effect must be small as evidenced by the flatness of the experimental efficiency variation with Mach number. It was assumed that maximum lift-drag ratio was attained at the reduced Mach numbers.

It can be seen that there is better agreement between the flight data and both sets of theoretical calculations at Mach numbers 0.85 and 0.90 (figs. 12(a) and 12(b)) than at Mach number 0.98 (fig. 12(c)). The flight data are in closer agreement with the authors' calculations at Mach number 0.98 than with the Aeroproducts calculations. One explanation for this difference is the amount of loss attributed to shock interference by Aeroproducts. The amount of this loss according to reference 13 is on the order of 4 to 5 percent.

The paucity of two-dimensional airfoil data in these regions of operation suggests that theoretically calculated values of propeller efficiency should be used with caution. It appears, however, from the fairly good agreement of flight data, wind-tunnel data, and theoretical calculations that, over the limited operating range of the turbine engine at high forward speeds, good efficiency is the case throughout. Small differences in power coefficient apparently have little effect on efficiency as the blade angle changes only minutely and continues to operate in a region of peak lift-drag ratio.

SUMMARY OF RESULTS

Results are presented of a flight investigation made with a propeller research vehicle, the McDonnell XF-88B airplane, to determine the aerodynamic characteristics of a typical supersonic propeller at speeds up to a flight Mach number of 1.01. The propeller was designed for a forward Mach number of 0.95, an advance ratio of 2.2, and a power coefficient of 0.22. At the design flight Mach number of 0.95, the propeller efficiency was measured to be 79 percent. At the maximum Mach number obtained (M = 1.01), the efficiency was 78 percent. Thrust distributions obtained by the use of a slipstream survey rake were of a uniform nature and showed no discontinuity typical of subsonic propellers when operated

under conditions which produce sonic local conditions. Limited theoretical calculations of efficiency indicate good agreement with the test results.

Langley Aeronautical Laboratory,
     National Advisory Committee for Aeronautics,
          Langley Field, Va., April 25, 1957.

APPENDIX A

DESCRIPTION OF TORQUEMETER

The electronic torquemeter used to determine power input to the
propeller gearbox is a modified commercial unit originally designed for
a 4,000-horsepower turbine engine. A general description of the com-
mercial unit is contained in reference 16. The commercial torquemeter,
although adequate for its original design purpose of an operational indi-
cating instrument, was inadequate as a research tool. It was therefore
necessary to modify extensively the unit to meet the exacting demands
of a research instrument. The description of the modified unit is given
herein. A breakdown of the torquemeter is shown in figure 5. The elec-
tronic torquemeter consists of three major units: (1) the drive-shaft
unit, (2) the pickup housing unit, and (3) the electronic amplifier unit.

The drive-shaft unit consists of two concentric shafts, which replace
the standard drive-shaft unit. The inner shaft (torque shaft) used to
transmit the torque from the engine to the gearbox twists in proportion
to the torque load. The outer shaft (reference shaft) is rigidly attached
to the torque shaft at the engine end and is free at the gearbox end.
The reference shaft rides on sleeve bearings over the torque shaft to
prevent lateral movements between the two shafts. At the gearbox end of
the drive-shaft unit, two rows of exciter teeth are mounted in tandem,
one row mounted on the reference shaft and one on the drive shaft. The
torque input to the gearbox varies the angular displacement between the
two tandem rows of teeth because of the twist of the torque shaft. A
calibration of the drive shaft as a function of static torque and angular
displacement was made prior to the installation in the aircraft.

The magnetic-pickup housing unit, which replaces the standard torque-
shaft housing, is attached rigidly to the engine and gearbox and surrounds
the torque-shaft unit. Mounted in the housing at the gearbox end directly
over the tandem rows of teeth are three magnetic pickups. Two are mounted
over the reference row of teeth (calibration and reference pickups) and
one over the torque row of teeth (torque pickup). As the teeth pass the
magnetic pickups, the change in the magnetic field is noted as an impulse.

The impulses from the magnetic pickups are passed to the electronic
unit where the impulses are clipped, sharpened, amplified, and passed
through a multivibrator circuit where the relative angular displacement
between impulses is converted to an electric current. This current is
passed to a recording galvanometer where it is recorded as a moving trace
line on film.

In order to measure torque input to the gearbox, the impulses from the reference pickup over the reference-teeth row and the one torque pickup over the torque-teeth row are utilized. The impulses from the calibration and reference pickups mounted over the reference-teeth row are used to adjust the torque output readings for sensitivity changes, amplifier lags, and magnetic-pickup lags.

The torque-shaft twist angle may be determined from the output readings by the following equation:

$$\frac{\theta}{12^{\circ}} = \frac{8.13^{\circ}}{12^{\circ}} - \left(\frac{RC - RT}{E}\right) - \left(\frac{\theta_{tare} + \theta_{T-C}}{12^{\circ}}\right) \tag{A1}$$

and the torque output may be determined by the equation

$$Q = K\theta$$

where

Q — torque delivered to propeller shaft

K — torque-shaft twisting constant determined from static torque tests (this value varies with operating temperature of torque shaft)

θ — phase-angle change between a reference and torque shaft due to power delivered to propeller shaft

θ_{tare} — phase angle due to initial angular displacement between reference and torque-teeth rows and between reference and torque magnetic pickups (included in this tare is gearbox load; this must be adjusted slightly for powers delivered to propeller shaft, as explained subsequently)

RC — galvanometer deflection due to reference pickup triggering the unit "on" and calibration pickup triggering the unit "off" (this signal includes amplifier lags and pickup lag between reference and calibration pickup)

RT — galvanometer deflection due to reference pickup triggering the unit "on" and torque pickup triggering the unit "off" (this signal includes amplifier lag and differential lag between reference and torque pickups)

E   sensitivity of instrument, that is, the galvanometer deflection
           with current "on" only (it is a representation of a 12° phase-
           angle difference without lags)

θ_{T-C} phase angle due to differential lags between calibration and
           torque magnetic pickups

The value of 8.13° used in equation (A1) is the angular displacement
between the reference and calibration magnetic pickups.

From equation (A1) it may be seen that, by knowing the torque out-
put, as in tests without a propeller, the relations contained in the

last bracket of the equation $\dfrac{\theta_{tare} + \theta_{T-C}}{12°}$ may be solved. Once this

value is known, the torque-shaft twist angle may be solved for under test
conditions through use of equation (A1).

It is of importance here to point out that the relation used to
determine torque automatically takes care of the amplifier lags and that
the pickup lags all cancel except the differential lags between the torque
and reference pickups. The amplifier lags in the past have changed in
an unpredictable manner; pickup lags, however, have not changed appre-
ciably except after an engine change.

Under actual test conditions, the values of E, RT, and RC are
automatically recorded every minute during a test. In addition to these
signals is the signal CR, which is the galvanometer deflection due to
the calibration pickup triggering the unit "on" and the reference pickup
triggering the unit "off." This signal also includes amplifier lag and
the differential pickup lags between reference and calibration pickup.
It can be seen that by the addition of RC and CR the value will be
in error from 12° by twice the amplifier lag difference, with the pickup
lag dropping out. Also, the difference of RC and CR will be in error
from 4.26° by twice the pickup differential lag between R and C pickups,
with the amplifier lags dropping out. This will enable a continuous check
of all variables in the system except a lag change in the torque magnetic
pickup (as previously stated, pickup lags have remained relatively
constant).

The torque as determined by the equation $Q = K\theta$ is actually the
torque delivered to the propeller shaft at zero torque load. In order
to determine the torque input to the propeller, the readings have to be
corrected for gearbox loads which vary with torque load. This correc-
tion is obtained from a factory test on a factory installed dynamometer.
The load at zero torque amounts to approximately 15 horsepower for the
3,600 rpm gearbox and 25 horsepower for the 1,700 rpm gearbox. This
load increases linearly by approximately 10 horsepower when 2,500 horse-
power is delivered to the propeller shaft. In addition, the operating

temperature of the torquemeter housing is measured to determine the
correction to apply for changes in the torsional modulus of elasticity
of the torque shaft. This change amounts to roughly 0.5-percent change
in torque readings per 30° F change in the shaft temperature.

REFERENCES

1. O'Bryan, Thomas C.: Flight Measurements of the Vibratory Bending and Torsion Stress on a Supersonic-Type Propeller for Flight Mach Numbers Up to 0.95. NACA RM L56D20a, 1956.

2. Hammack, Jerome B., and O'Bryan, Thomas C.: Flight Measurements of Section Efficiency, Thrust, and Power of a Supersonic-Type Propeller at Mach Numbers to 0.9. NACA RM L55I21, 1956.

3. Hine, E. K.: Design Considerations of the Propellers and Equipment for the XF-88B Propeller Flight Research Vehicle. Rep. No. C-2437, Curtiss-Wright Corp., Propeller Div. (Caldwell, N. J.), June 3, 1953.

4. Amatt, H.: Design Strength of the Curtiss C6325D-B2, C6425D-A2, C532S-E304, and C542S-B32 Hubs. Rep. No. C-2345, Curtiss-Wright Corp., Propeller Div. (Caldwell, N. J.), Dec. 10, 1951.

5. Smith, C. B., and Giarratana, S. A.: The Supersonic Propeller. Concluding Report. Rep. R-12004-03, United Aircraft Corp., Res. Dept., Apr. 23, 1948.

6. Borst, H. V.: Aerodynamic Study of the Theory and Performance of Supersonic Propellers. Rep. No. C-2044B, Curtiss-Wright Corp., Propeller Div. (Caldwell, N. J.), Mar. 29, 1949.

7. Hammack, Jerome B.: The Aerodynamic Design of Supersonic Propellers From Structural Considerations. NACA TN 2851, 1952.

8. Vogeley, A. W.: Flight Measurements of Compressibility Effects on a Three-Blade Thin Clark Y Propeller Operating at Constant Advance-Diameter Ratio and Blade Angle. NACA WR L-505, 1943. (Formerly NACA ACR 3G12.)

9. Pankhurst, R. C.: Airscrew Thrust Grading by Pitot Traverse: Allowance for Rotation of Slipstream at High Rates of Advance. R. & M. No. 2049, British A.R.C., 1945.

10. Hine, E. K.: Precision Blade Angle Indicator. Rep. No. C-2420, Curtiss-Wright Corp., Propeller Div. (Caldwell, N. J.), Mar. 2, 1953.

11. Hammack, Jerome B., Windler, Milton L., and Scheithauer, Elwood F.: Flight Investigation of the Surface-Pressure Distribution and the Flow Field Around a Conical and Two Spherical Nonrotating Full-Scale Propeller Spinners. NACA TN 3535, 1955.

12. Klawans, Bernard B., and Vogeley, Arthur W.: A Cascade—General-
    Momentum Theory of Operation of a Supersonic Propeller Annulus.
    NACA RM L52J06, 1953.

13. Stolp, P. C.: Aerodynamic Design Study of the A39SFN-125 Propeller.
    Eng. Rep. No. 689, Aeroproducts Div., General Motors Corp. (Dayton,
    Ohio), May 19, 1954.

14. Jacobson, D. H.: Performance Analysis of the A39SFN-125 Supersonic
    Type Propeller. Eng. Memo. Rep. No. 913, Aeroproducts Div.,
    General Motors Corp. (Dayton, Ohio), Jan. 15, 1951. (Rev. Feb. 11,
    1954.)

15. Daley, Bernard N., and Dick, Richard S.: Effect of Thickness, Camber,
    and Thickness Distribution on Airfoil Characteristics at Mach Num-
    bers Up to 1.0. NACA TN 3607, 1956. (Supersedes NACA RM L52G31a.)

16. Anon.: Installation & Overhaul Instruction. TP-95-C, Allison Div.,
    General Motors Corp., Apr. 9, 1953.
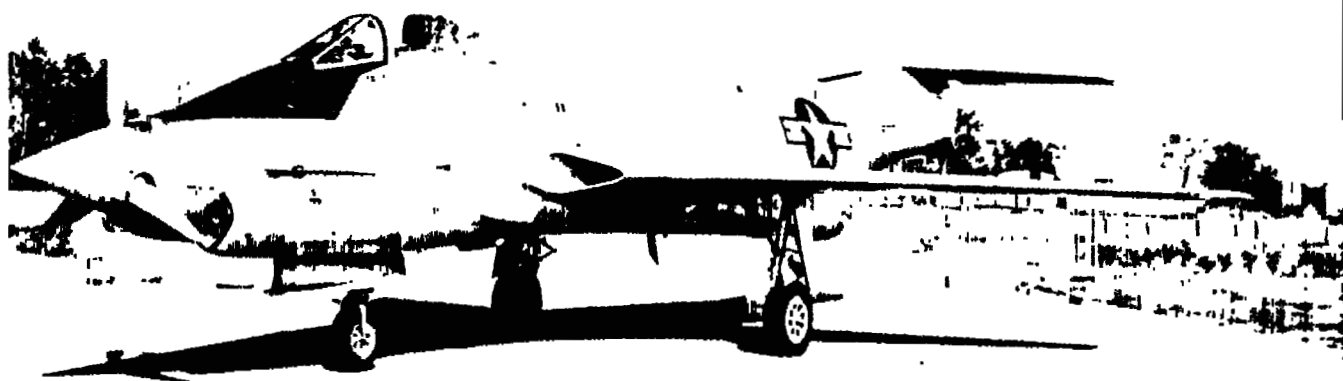
Figure 1.- The McDonnell XF-88B propeller research vehicle with test propeller.   L-91635
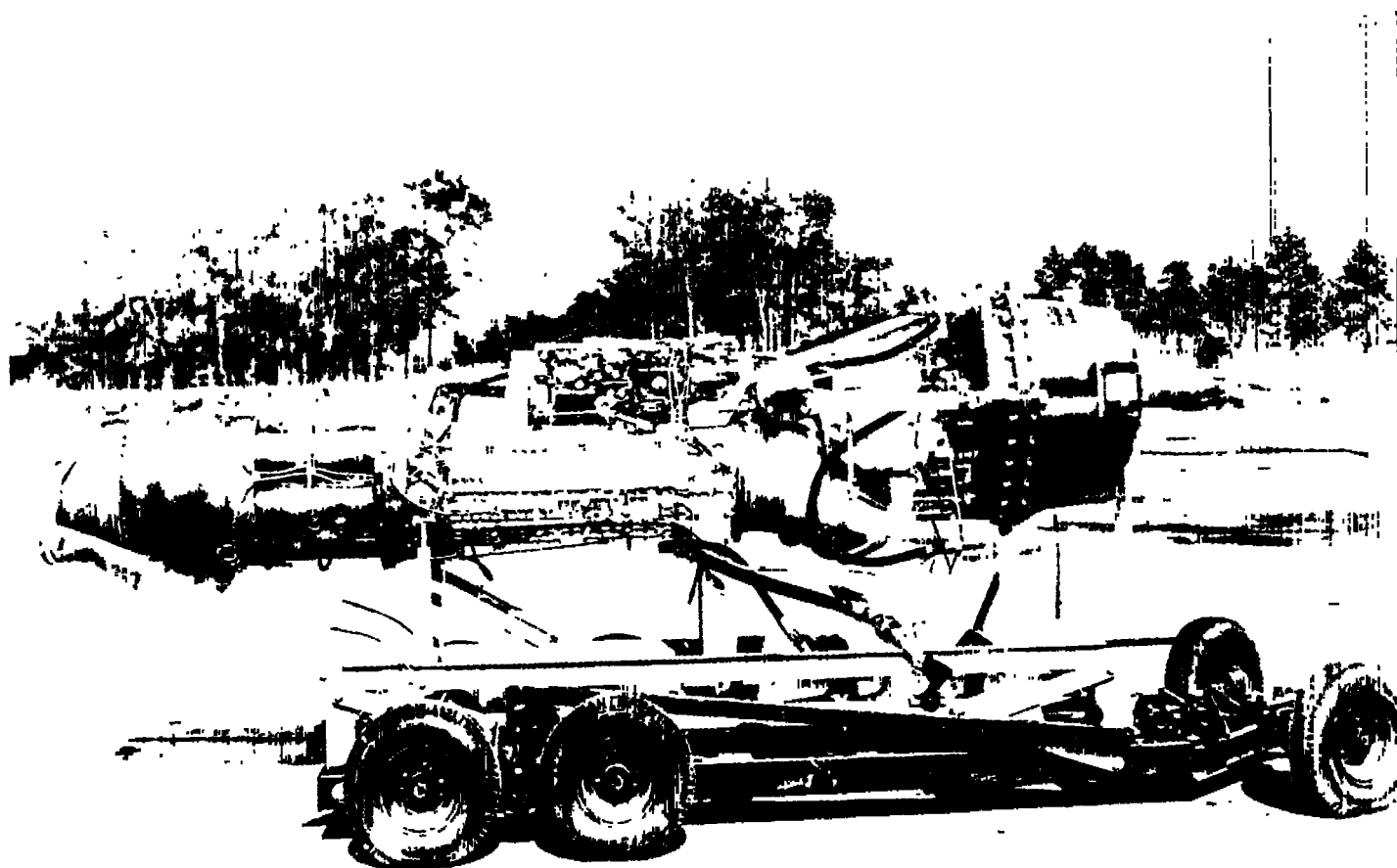
L-81971

Figure 2.- The T-38 turboprop engine showing the power section and special gearbox.
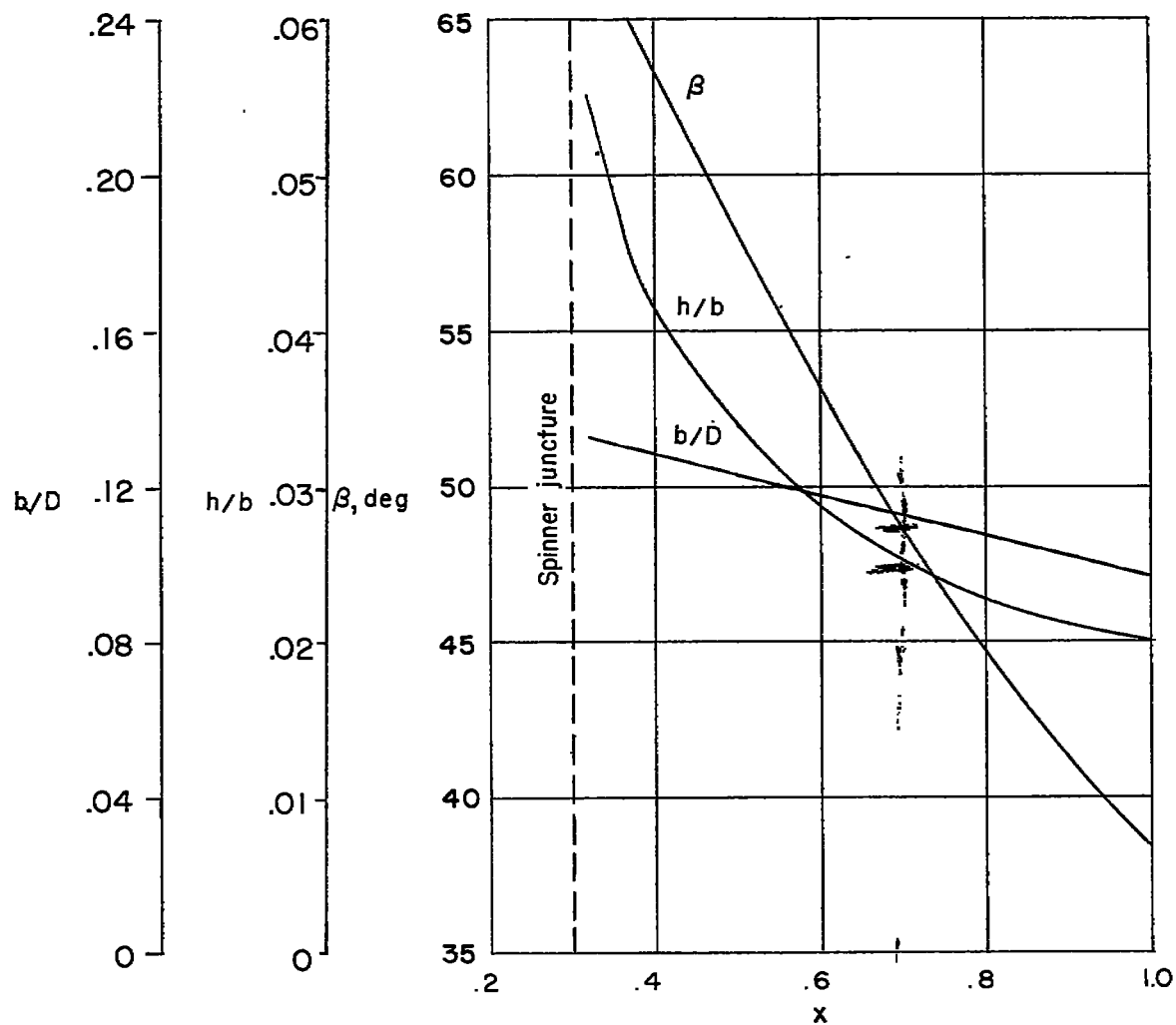
Figure 3.- Blade-form curves of the test propeller.

Forward instrument compartment
12-capsule recording manometers (9)
Torque recorder
Electronic propeller governor
Fuel-control amplifier

Blade-stress indicator (2)
Blade-angle indicator
Propeller governor control
Instrument switches
Engine overspeed warner, indicator and shut-down switch

Aft. instrument compartment
Single-component recording accelerometers (2)
18-Channel oscillograph
Airspeed-altitude recorder
Blade "Flutter" amplifiers
Torquemeter amplifier and power supply
Root blade-angle recorder
Root blade-angle amplifier
Tachometer recorder
Batteries, inverter, etc.
Timer ($\frac{1}{10}$ second)

Propeller wake survey rakes
(each side)
Total pressure probes (46)
Static pressure probes (46)
Yaw angle probes (46)
Wake temperature rise (20)

Free-floating spinner
Research propeller (2 to 4 blades)
Root blade-angle transmitter
Strain gages (24)
Slip-ring pineapple

T-38 operating console
(switches, oil pressure, etc.)

Ballast
Pilot's airspeed head
Angle-of-attack transmitter
Yaw transmitter
Camera
Radar altimeter scope
J-34 afterburners (2)
Radar altimeter antennae
Free-air temperature bulb
Research airspeed head (airspeed, altitude)

Oil-cooler inlet
Reduction gear box
Air inlet
Torque transmitter

T-38 exit nozzle
Turbine inlet-temp probes
Fuel-flow transmitter
Throttle position transmitter
T-38 propeller turbine
Tachometer generator

L-57-1077

Figure 4.- Instrumentation layout on the McDonnell XF-88B airplane.

Calibration pickup

Torque pickup

Reference pickup

Damper bearing

Sleeve bearing

Exciter teeth

Pickup housing

Reference shaft

Torque shaft

Gearbox end

Engine end
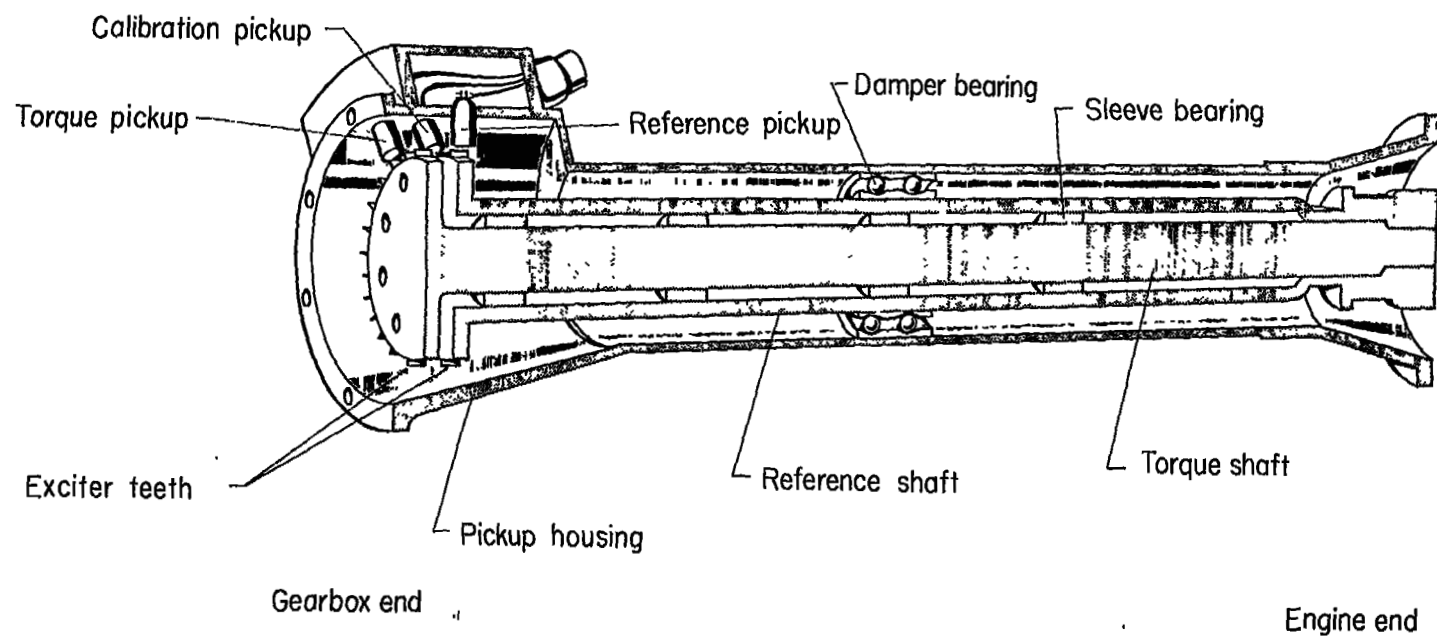
Figure 5.- The Allison torquemeter.
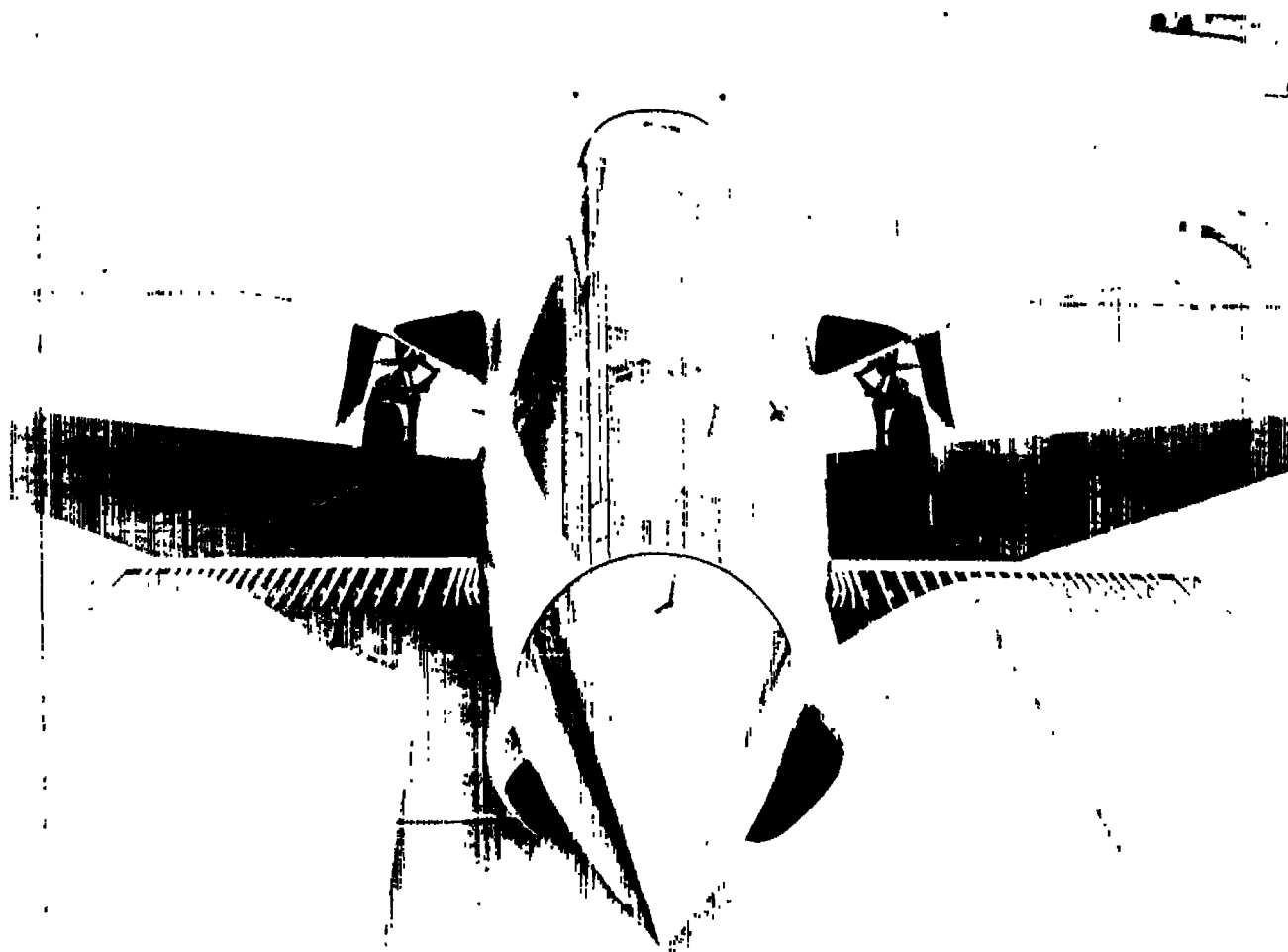
L-94744

Figure 6.- The slipstream survey rake mounted on the McDonnell XF-88B propeller research vehicle for calibration flights.
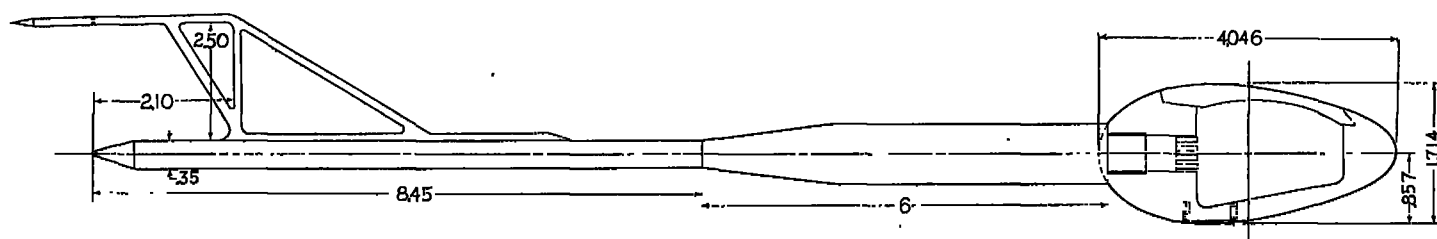
Figure 7.- Typical survey rake probe and support strut. All dimensions are in inches.
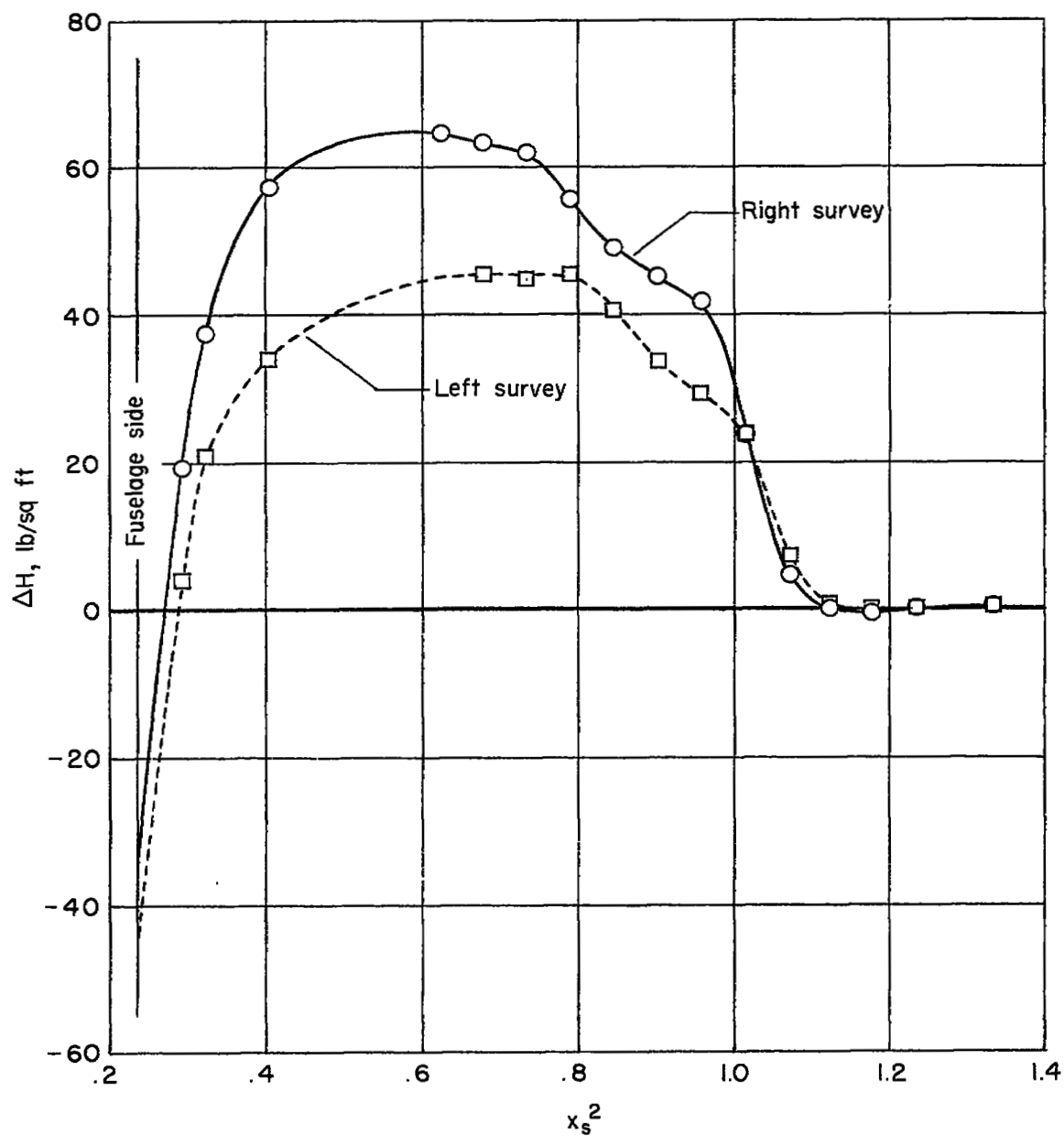
(a) M = 0.60, J = 1.501, C_P = 0.188, M_t = 1.392.

Figure 8.- Total-pressure grading curves as measured with the slipstream survey rake.
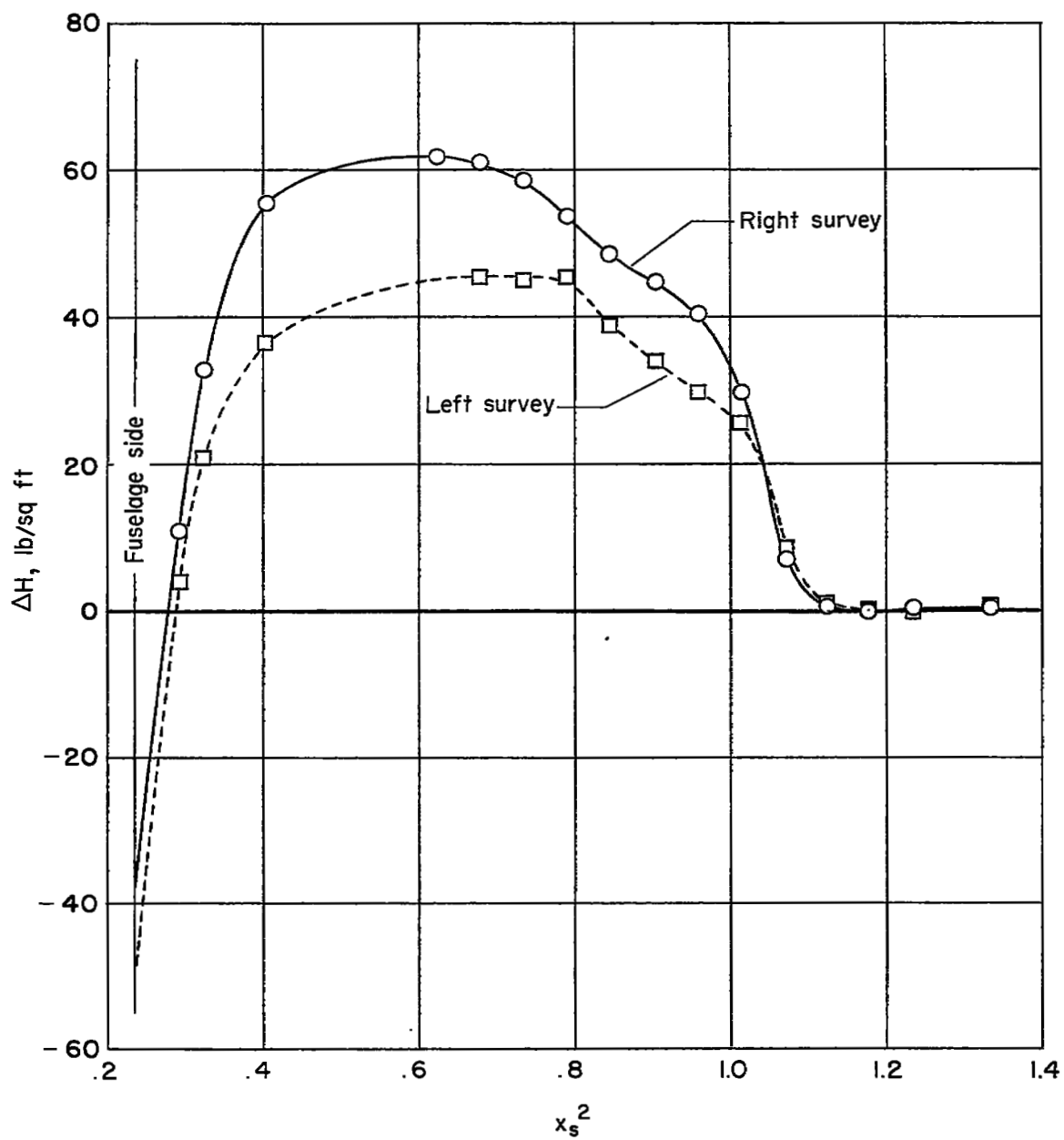
(b) M = 0.65, J = 1.626, C_P = 0.195, M_t = 1.414.

Figure 8.- Continued.
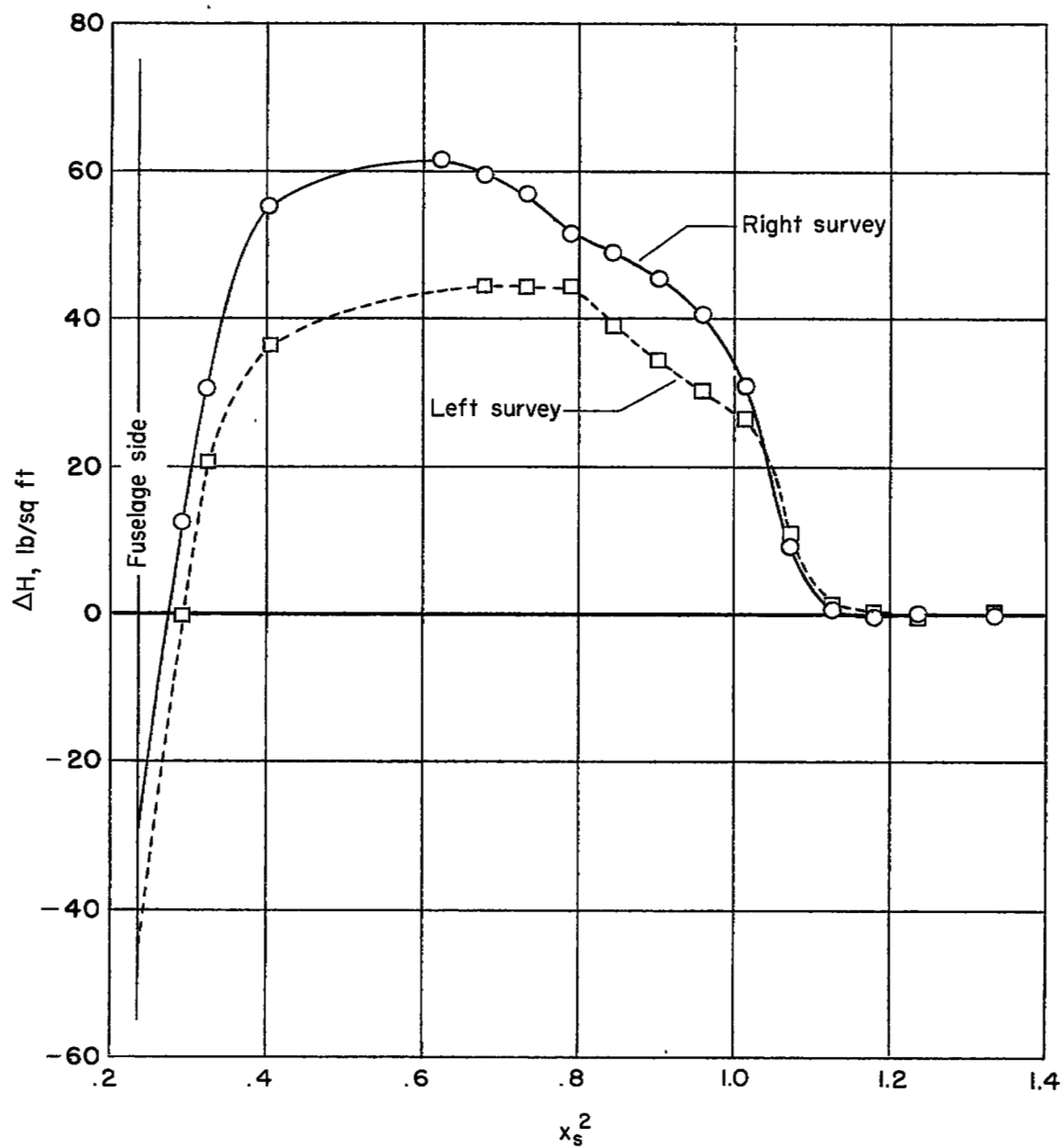
(c) M = 0.70, J = 1.756, Cp = 0.204, M_t = 1.435.

Figure 8.- Continued.
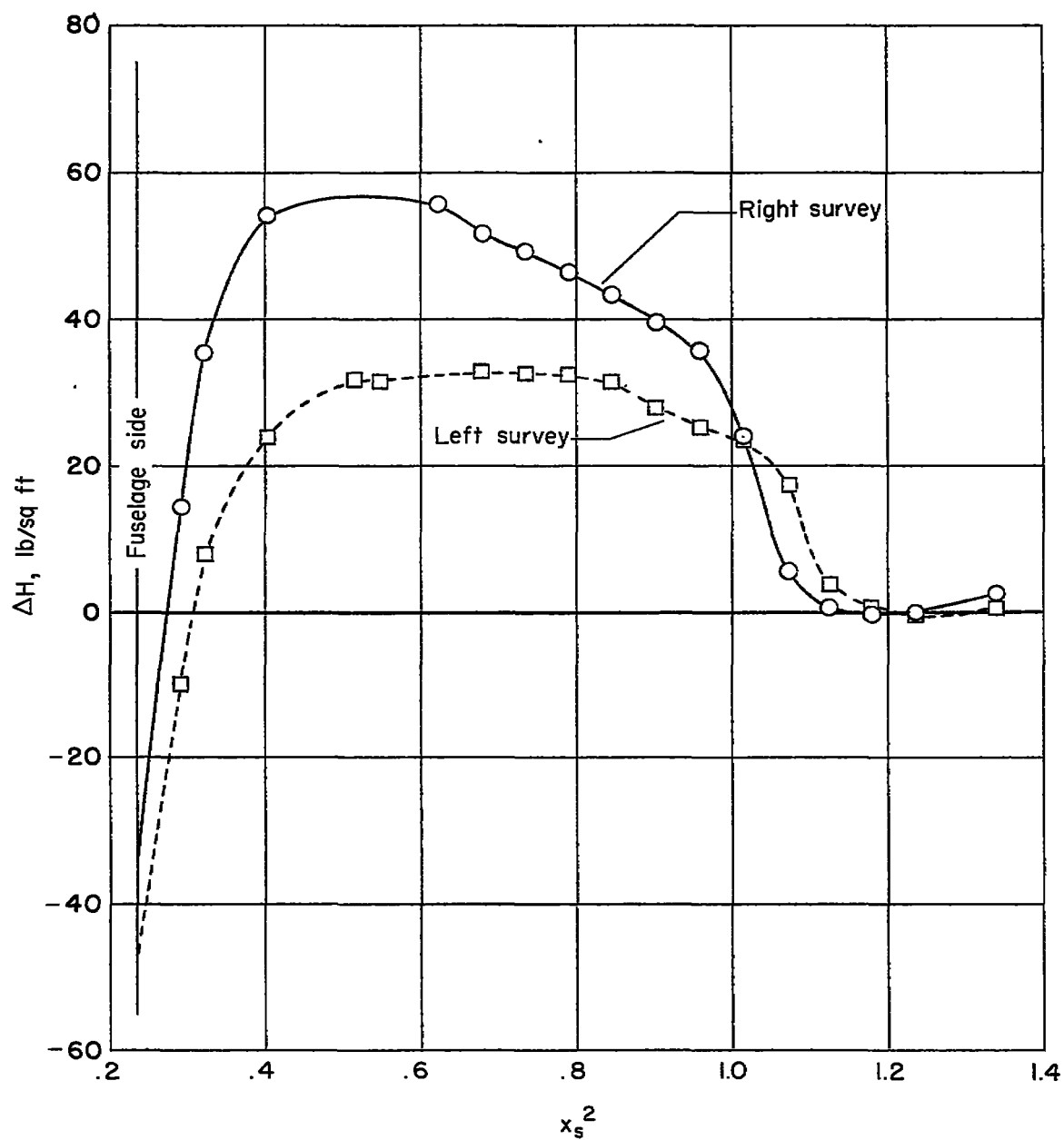
(d) M = 0.75,   J = 1.831, C_P = 0.203, M_t = 1.490.

Figure 8.- Continued.
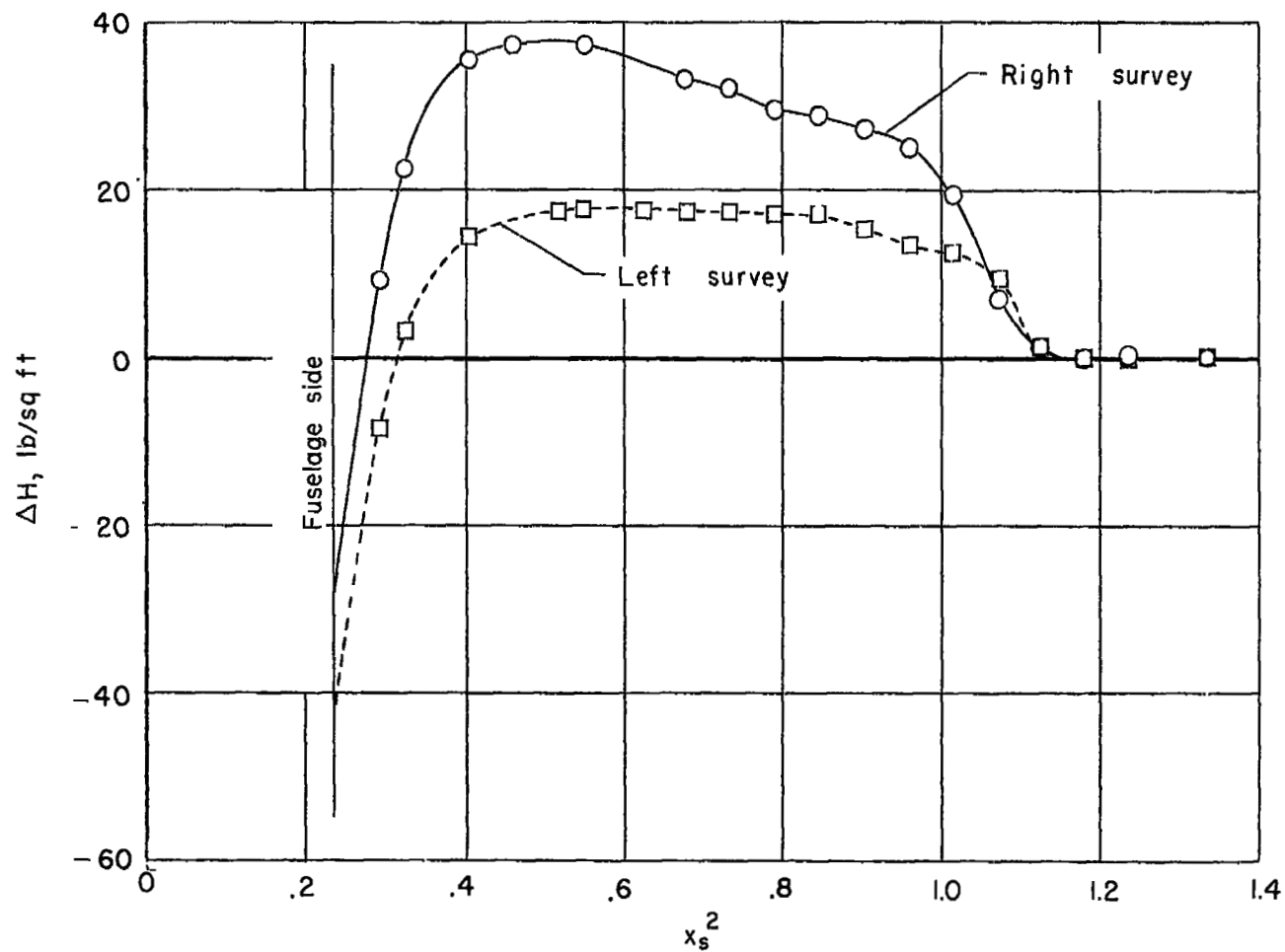
(e) M = 0.80, J = 1.834, C_P = 0.184, M_t = 1.586.

Figure 8.- Continued.
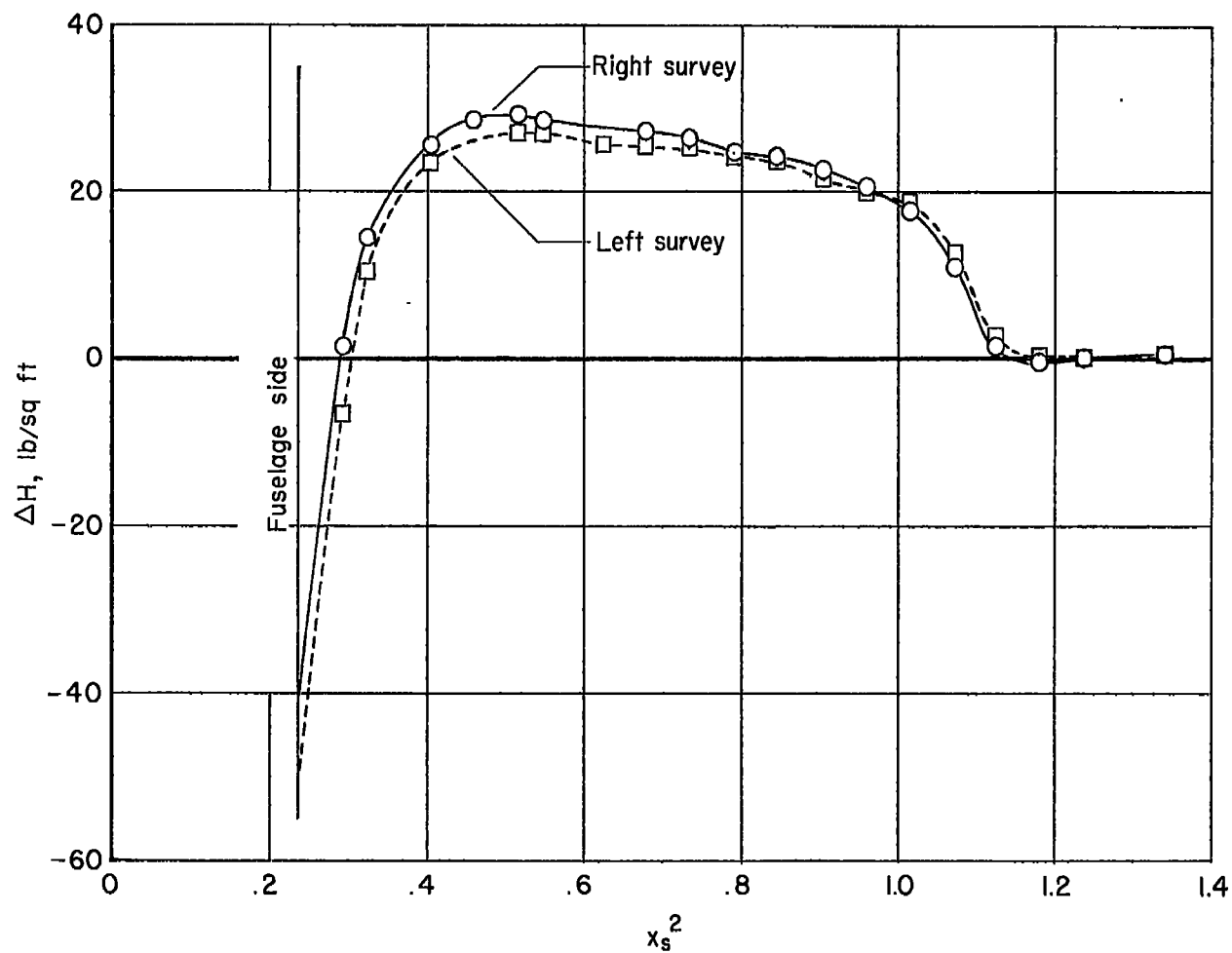
(f) M = 0.85, J = 1.946, Cp = 0.186, M_t = 1.614.

Figure 8.- Continued.
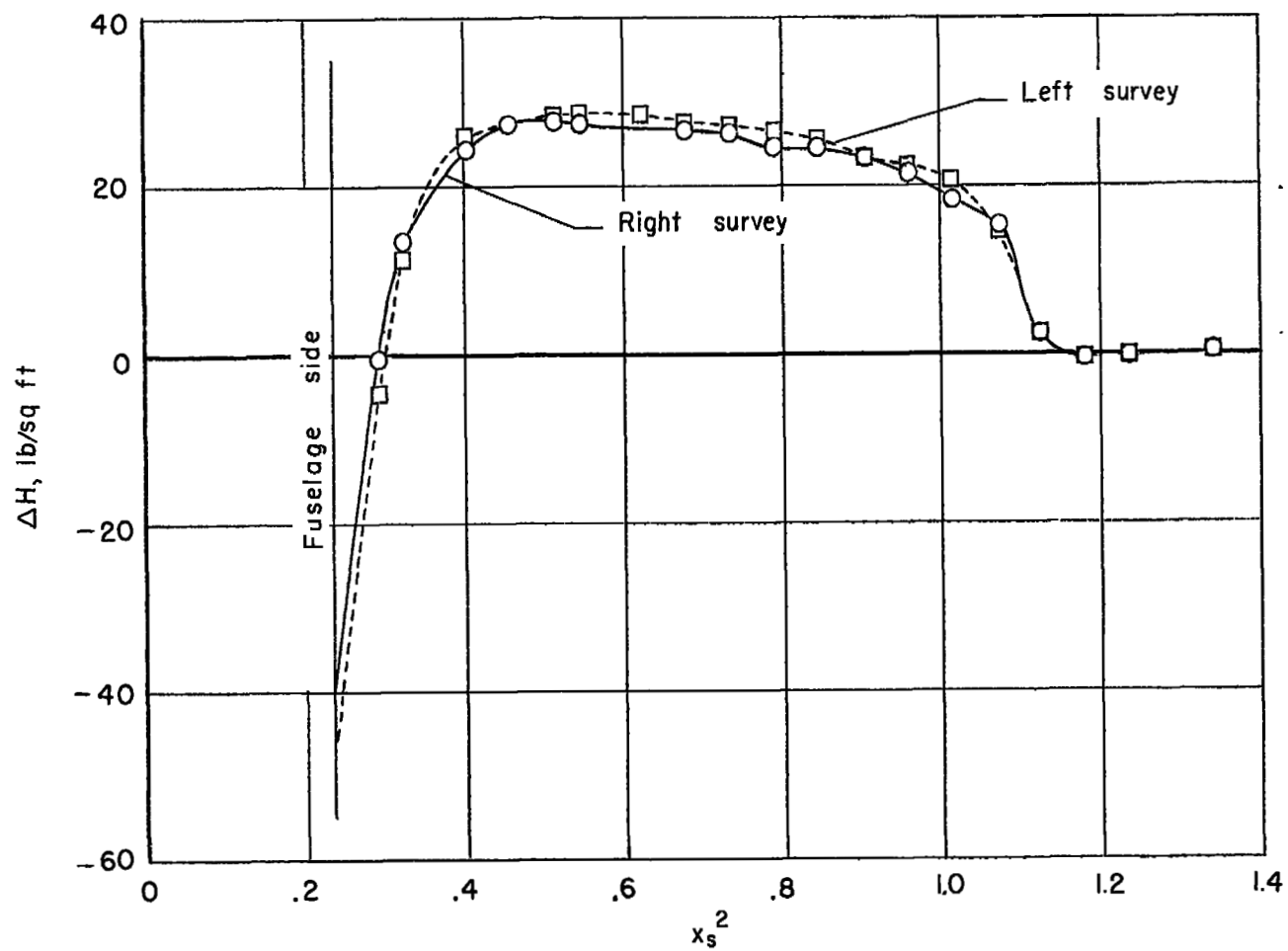
(g) $M = 0.90$, $J = 2.052$, $C_p = 0.189$, $M_t = 1.646$.

Figure 8.- Continued.
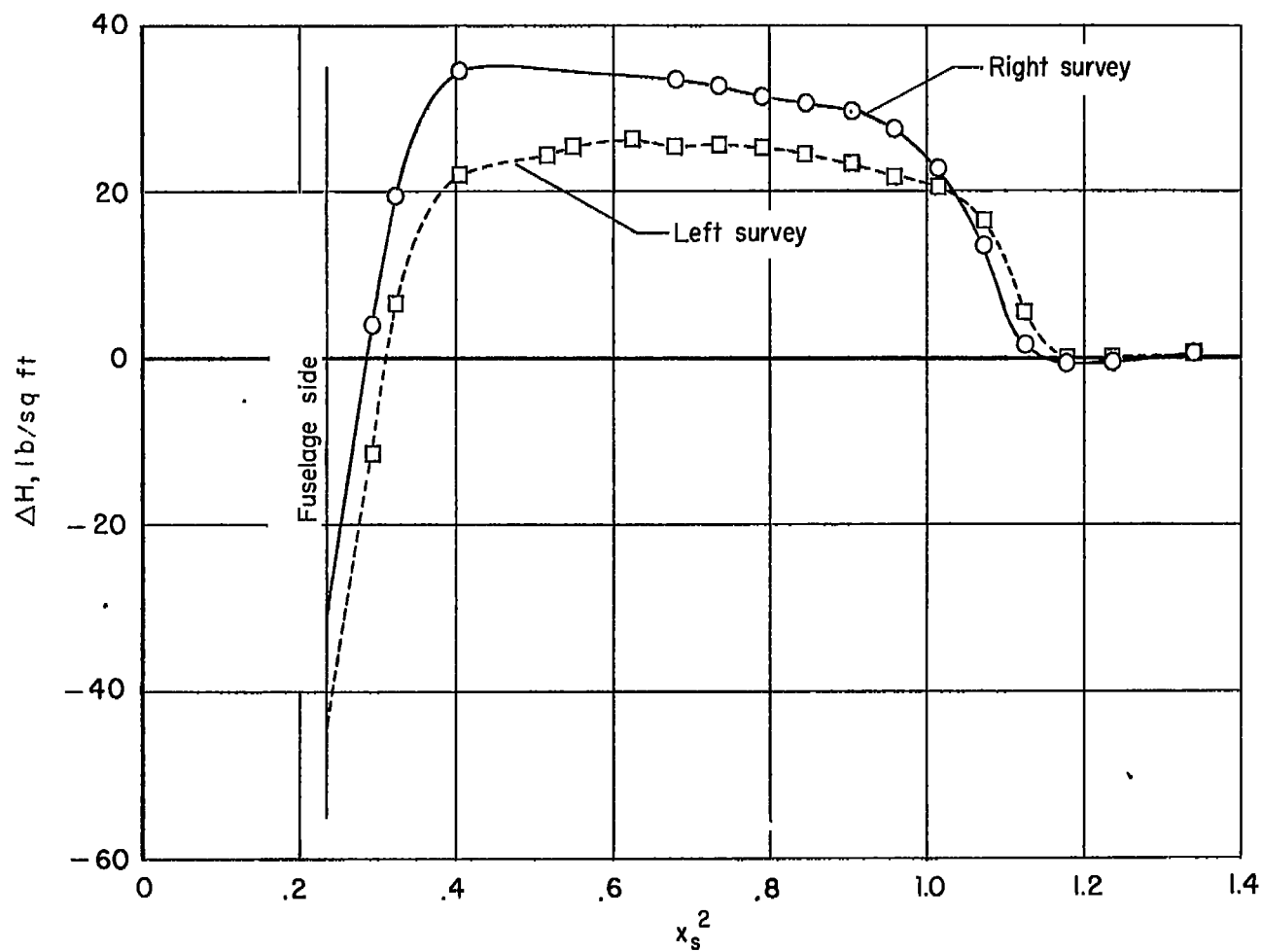
(h) M = 0.95, J = 2.191, Cp = 0.204, Mt = 1.661.

Figure 8.- Continued.
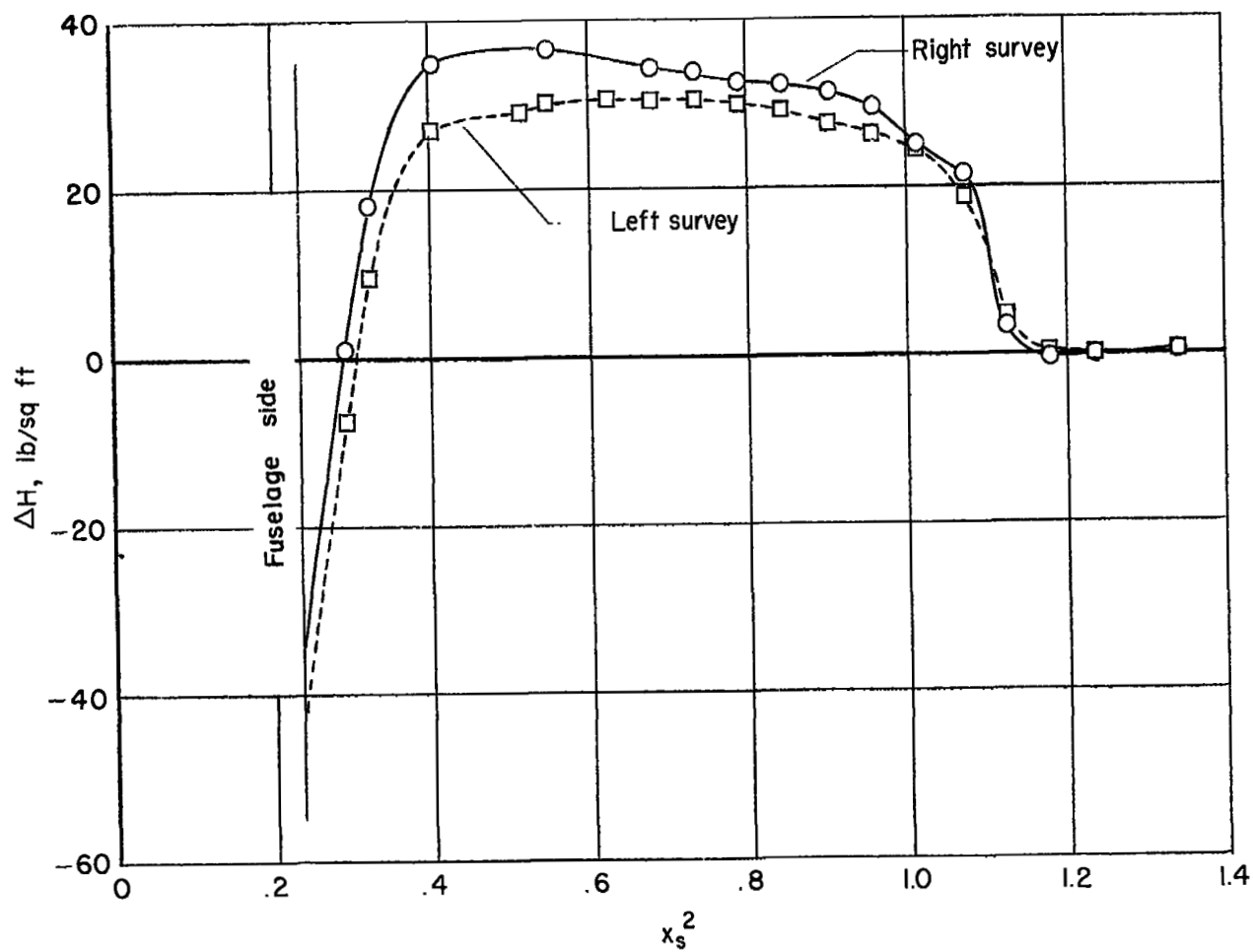
(i) M = 0.97,   J = 2.271,   C_P = 0.210,   M_t = 1.656.

Figure 8.- Continued.
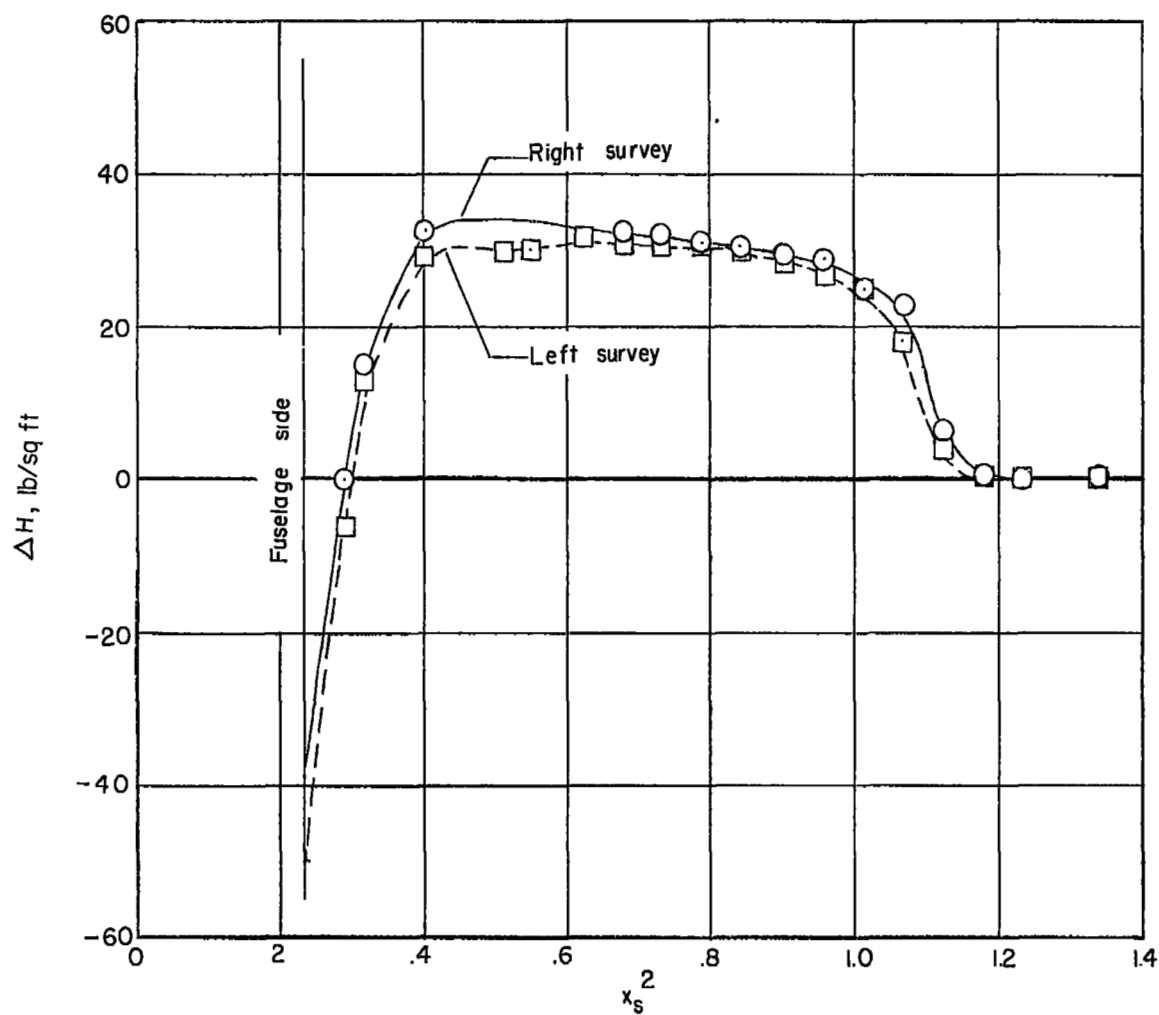
(j) M = 1.01, J = 2.35, C_P = 0.226, M_t = 1.689.

Figure 8.- Concluded.
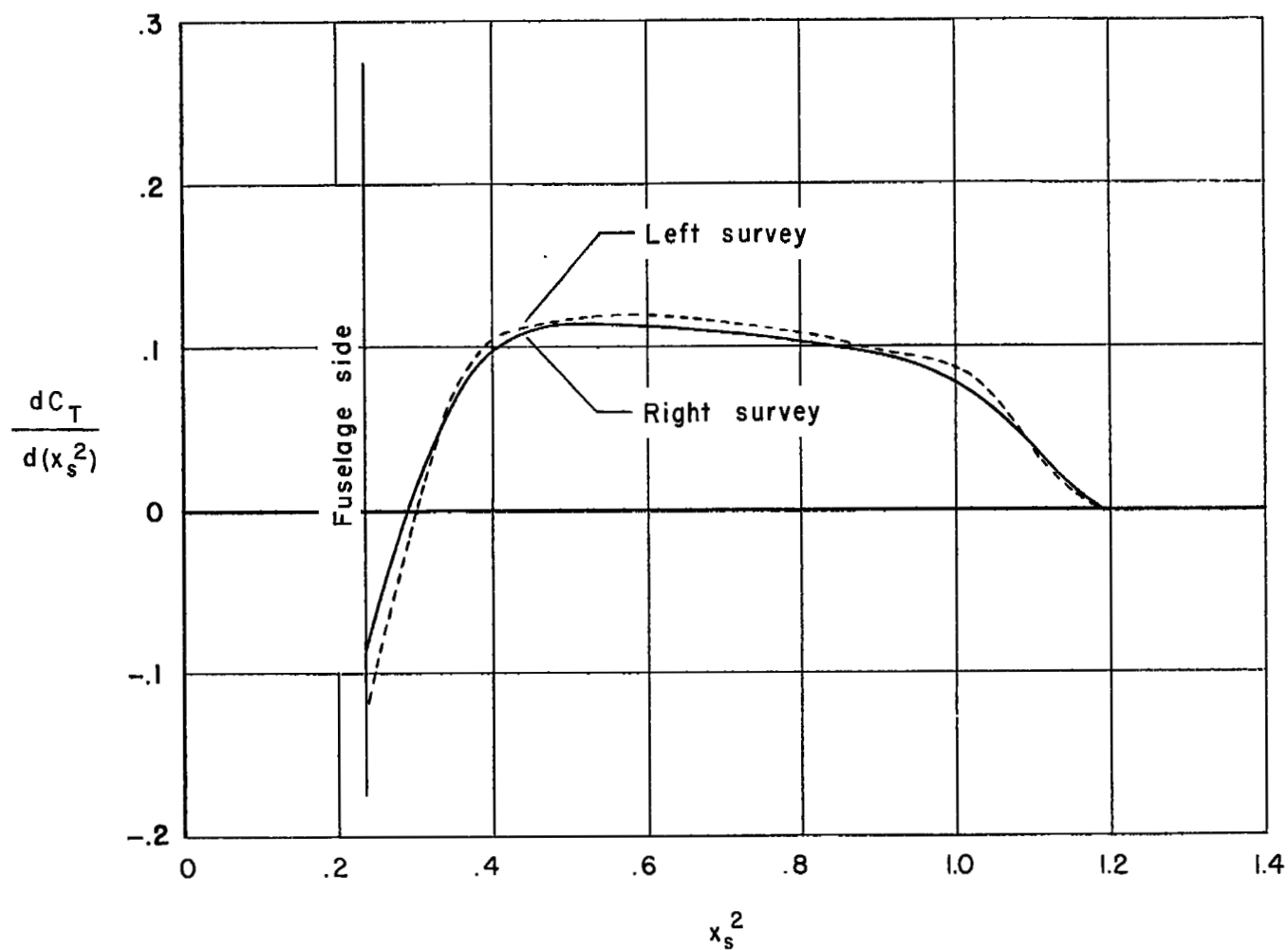
(a) M = 0.90,   J = 2.052, C_P = 0.189, M_t = 1.646.

Figure 9.- Thrust distributions of the test propeller and conical spinner.
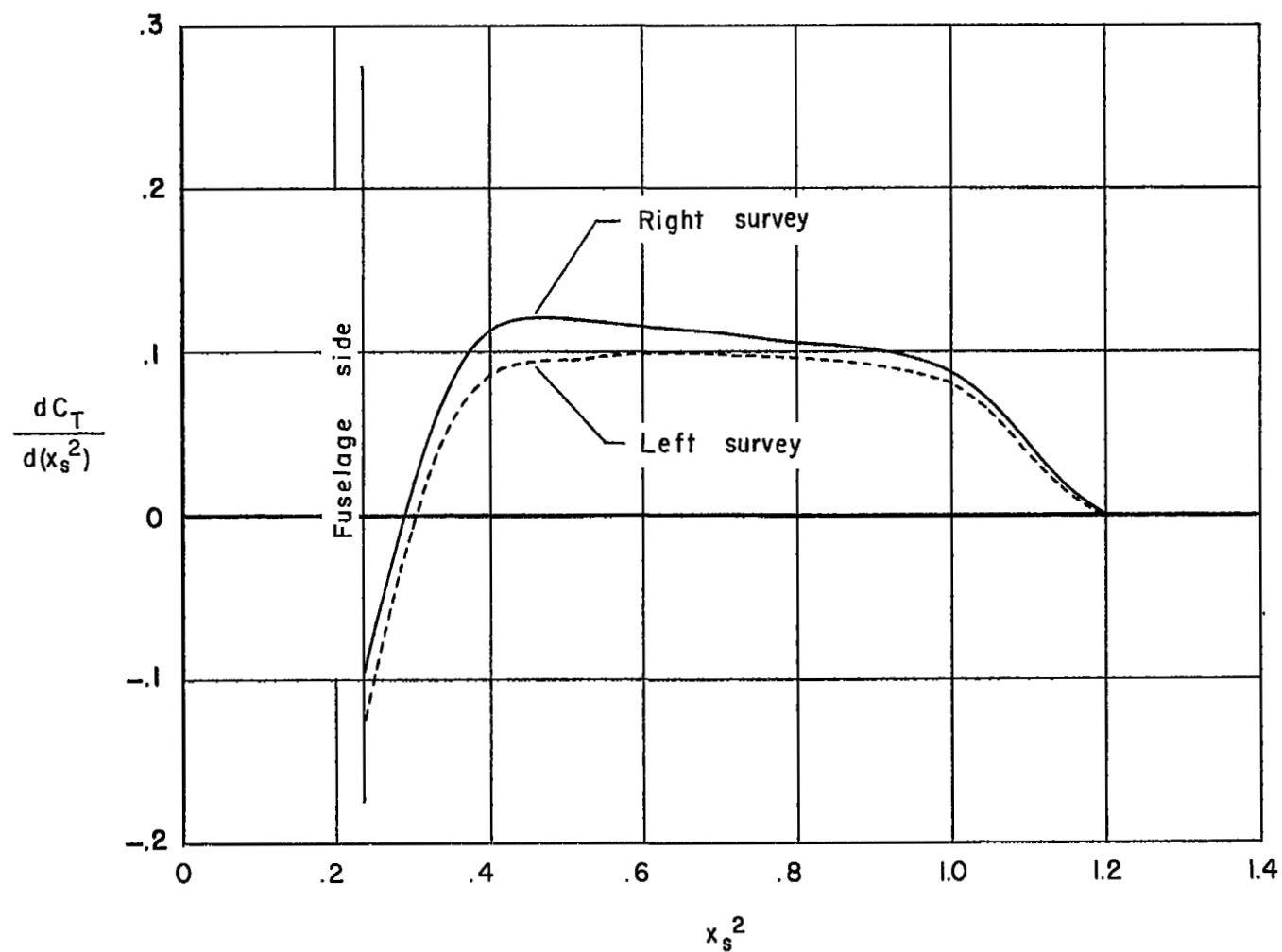
(b) M = 0.97, J = 2.271, C_p = 0.210, M_t = 1.656.

Figure 9.- Concluded.
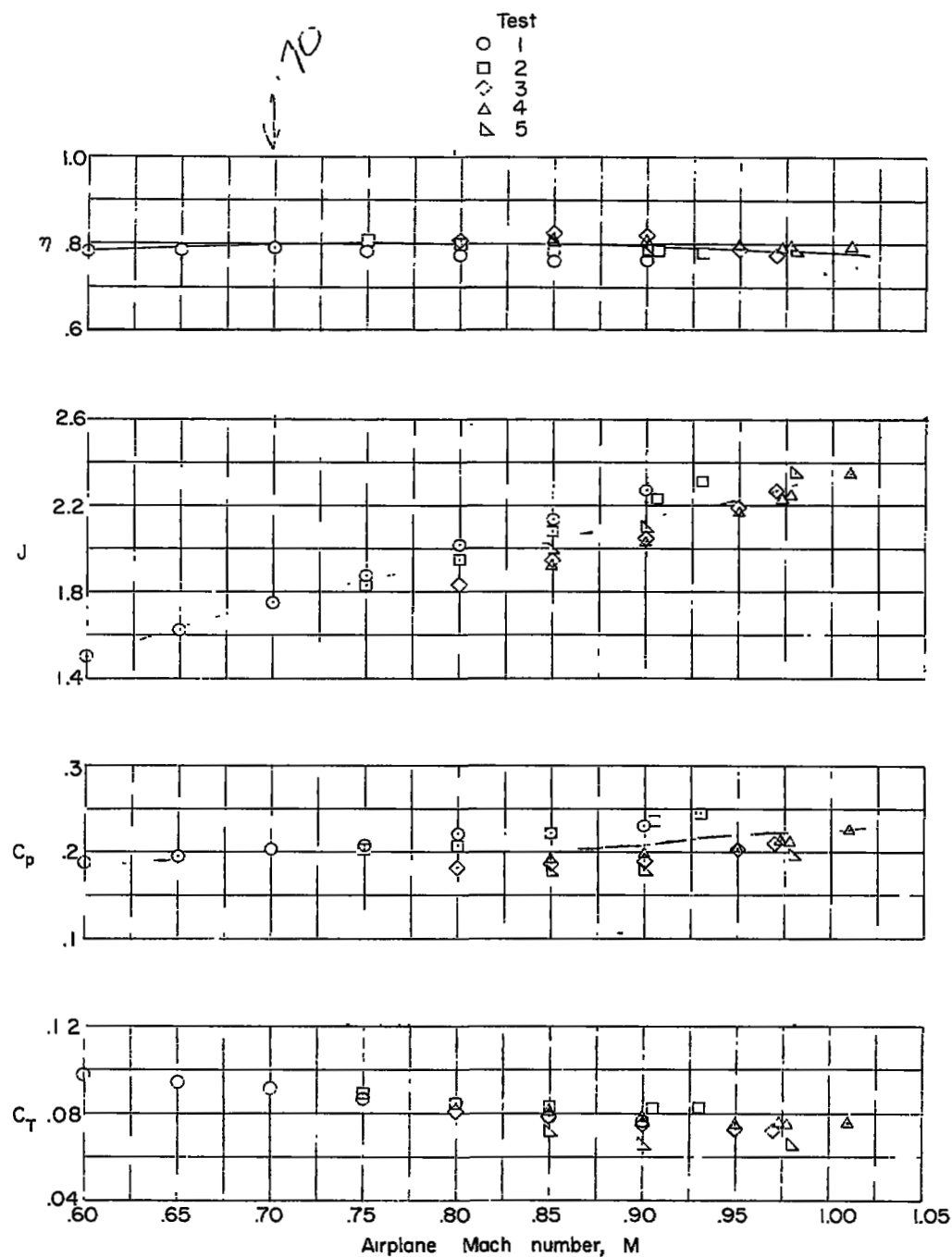
Figure 10.- Performance characteristics of the test propeller mounted on the XF-88B airplane up to Mach number 1.01.
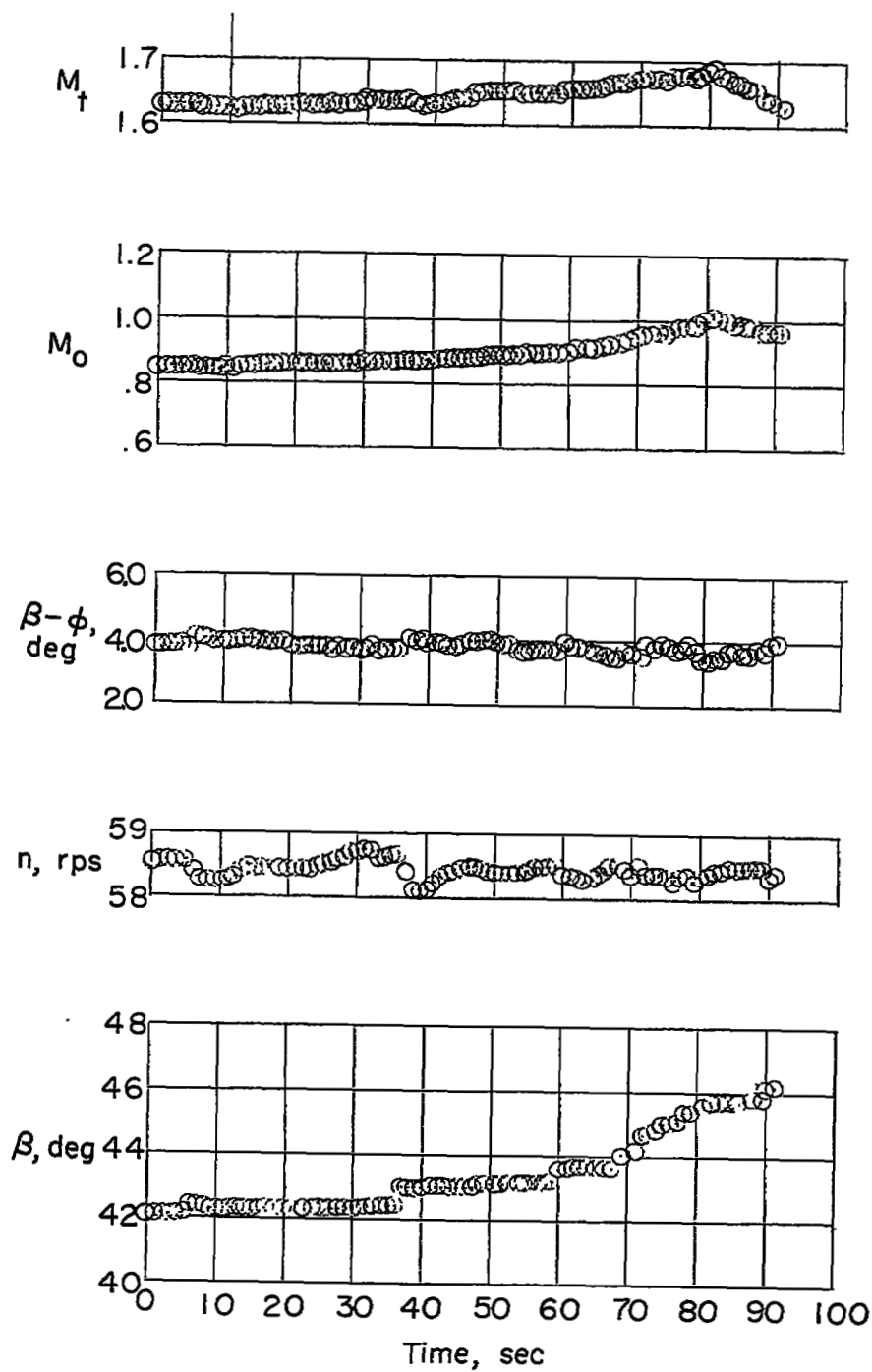
Figure 11.- Time history of propeller operation during a typical test flight.

(a) M=.85.

(b) M=.90.

(c) M = .98.
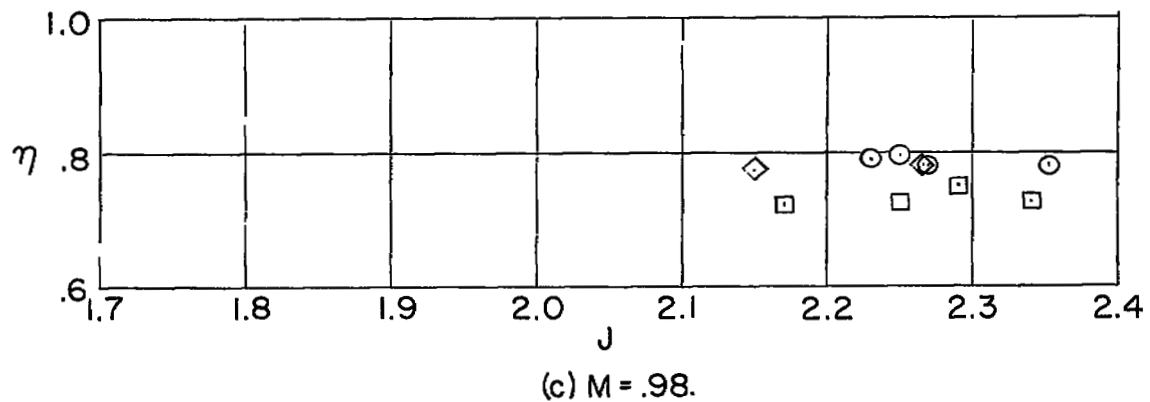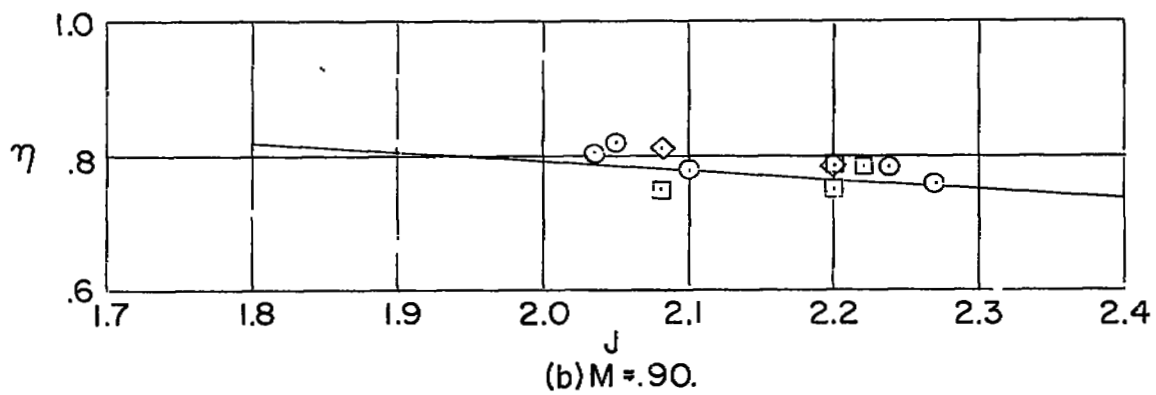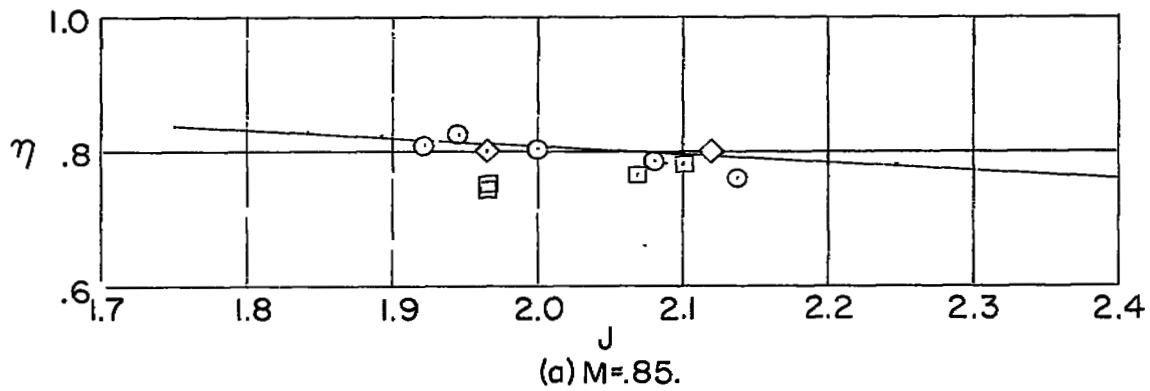
○ Flight tests
□ Aeroproducts calculations
◇ Authors' calculations
─── Envelope of Cornell data

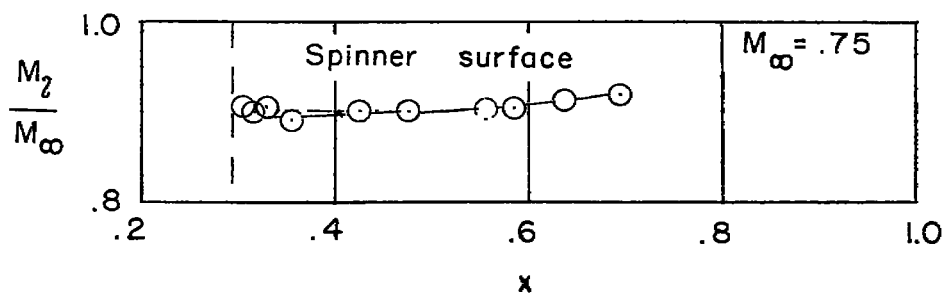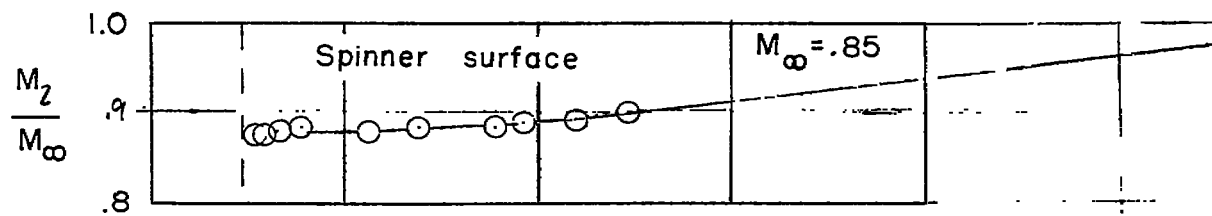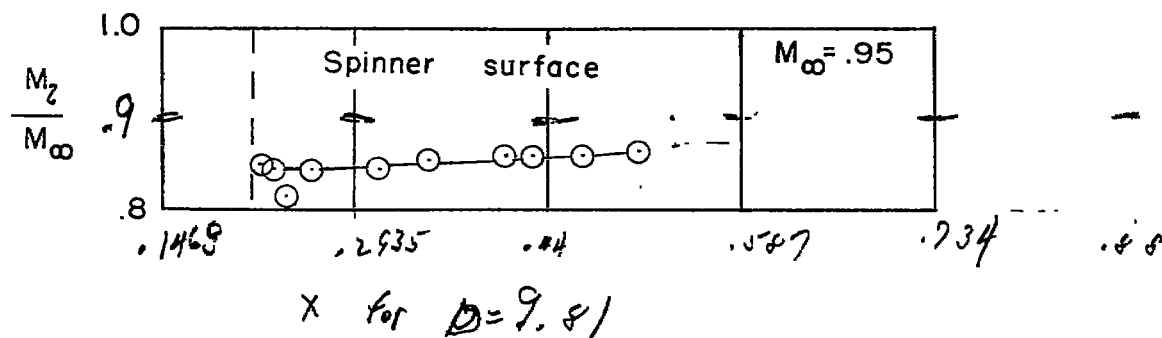Figure 12.- Comparison of experimental results with theoretical calculations and other data.

D= 9.2

X for D= 9.81

Figure 13.- Alteration in flow velocity caused by conical spinner.